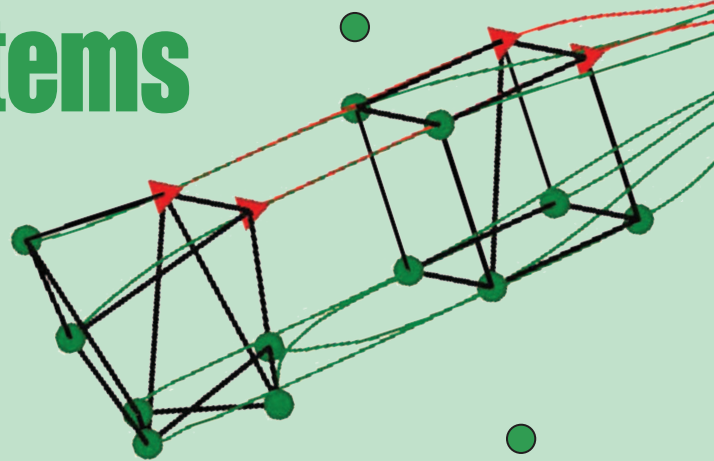


# Bearing Rigidity Theory and Its Applications for Control and Estimation of Network Systems



## LIFE BEYOND DISTANCE RIGIDITY

SHIYU ZHAO and DANIEL ZELAZO

**D**istributed control and location estimation of multiagent systems have received tremendous research attention in recent years because of their potential across many application domains [1], [2]. The term *agent* can represent a sensor, autonomous vehicle, or any general dynamical system. Multiagent systems are attractive because of their robustness against system failure, ability to adapt to dynamic and uncertain environments, and economic advantages compared to the implementation of more expensive monolithic systems.

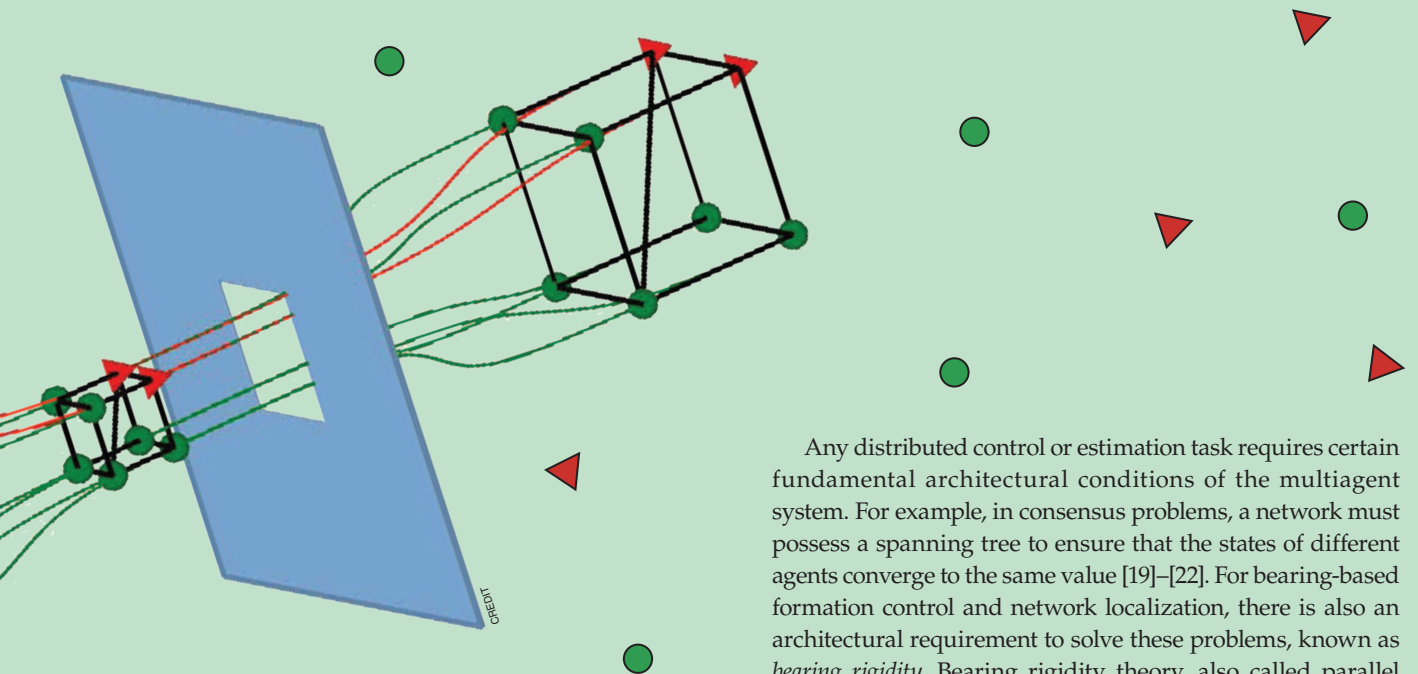
Formation control and network localization are two fundamental tasks for multiagent systems that enable them to perform complex missions. The goal of formation control is to direct each agent using local information from neighboring agents so that the entire team forms a desired spatial geometric pattern (see [2] for a recent survey on formation control). While the notion of a formation as a geometric pattern has a natural meaning for robotic systems, it may also correspond to more abstract configurations for the system state of a team of agents. The goal of network localization is to estimate the location of each agent in a network using locally sensed or communicated information from neighboring agents [3]–[6]. Network localization is usually the first step that must be completed before a sensor network provides other services, such as positioning mobile robots or monitoring areas of interest.

For a formation control or network localization task, the type of information available to each agent is an important

factor that determines the design of the corresponding control or estimation algorithms. Most of the existing approaches for formation control assume that each agent can obtain the relative positions of its nearest neighbors. To obtain these in practice, each agent can measure its own absolute position using a GPS, for example, and then share it with neighbors via wireless communications. This method is, however, not applicable when operating in GPS-denied environments, such as indoors, underwater, or in deep space. Furthermore, the absolute accuracy of the GPS may not meet the requirements of high-accuracy formation control tasks. Rather than relying on external positioning systems like the GPS, each agent can use onboard sensors to sense their neighbors.

Optical cameras are widely used onboard sensors for ground and aerial vehicles to achieve various sensing tasks because of their low-cost, lightweight, and low-power characteristics. It is notable that optical cameras are inherently bearing-only sensors. Specifically, once a target has been recognized in an image, its bearing relative to the camera can be calculated immediately from its pixel coordinate based on the pinhole camera model [7, Sec. 3.3].

As a comparison, the range from the target to the camera is more complicated to obtain because it requires additional geometric information about the target and extra estimation algorithms, which may significantly increase the complexity of the vision-sensing system. Although stereo cameras can be used to estimate the range of a target by triangulating the target's bearings [8], the estimation accuracy degenerates rapidly as the range of the target increases because of the short baseline between the two cameras.



Since it is easy for vision to measure bearings (but relatively difficult to obtain accurate range information), vision can be effectively modeled as a bearing-only sensing approach in multiagent formation control [9], [10]. In addition to cameras, other types of sensors, such as passive radars, passive sonars, and sensor arrays, are able to measure relative bearings [5], [11], [12].

When each agent is able to access only the bearings relative to their neighbors, two strategies can be adopted to achieve formation control or network localization. The first uses bearings to estimate relative positions. This strategy leads to coupled control and estimation problems whose global stability is difficult to prove (see, for example, [13]). Moreover, the estimation of relative positions depends on an observability condition requiring the relative motion of each pair of neighboring agents to satisfy certain conditions [14]. Although this observability condition can be achieved in certain applications (such as bearing-only circumnavigation [15]–[18]), it is difficult to satisfy in general formation control tasks where all agents are supposed to form a target formation with no relative motions among the agents. This observability condition is also not satisfied in network localization because all of the sensors are stationary.

The second strategy, which is the focus of this article, is to directly apply bearings in formation control or network localization without estimating relative positions. This strategy does not require relative position estimation but instead calls for designing new control and estimation algorithms that utilize only bearing measurements.

As discussed in “Summary,” the purpose of this article is to provide a tutorial overview of recent advances in the area of bearing-based formation control and network localization. The first problem addressed here is to understand when formation control or network localization problems can be solved using only interneighbor bearing measurements.

Any distributed control or estimation task requires certain fundamental architectural conditions of the multiagent system. For example, in consensus problems, a network must possess a spanning tree to ensure that the states of different agents converge to the same value [19]–[22]. For bearing-based formation control and network localization, there is also an architectural requirement to solve these problems, known as *bearing rigidity*. Bearing rigidity theory, also called parallel rigidity theory in the literature, was originally introduced for computer-aided design [23] and has received increasing attention in recent years because of its important applications in bearing-based control and estimation problems [24]–[28]. Bearing rigidity theory investigates the conditions where the geometric pattern of a network is uniquely determined if the bearing of each edge in the network is fixed.

Bearing rigidity theory can be interpreted as a theory analogous to the classic rigidity theory based on interneighbor distances, which is referred to as *distance rigidity theory* in this article. Classic distance rigidity theory studies the conditions where the geometric pattern of a network is uniquely determined if the length (distance) of each edge in the network is fixed. It is a combinatorial theory for characterizing

## Summary

The problem of distributed control and estimation for multiagent systems with limited sensing capabilities is a practical challenge motivated by incomplete and imperfect sensing. This article addresses an important case where each agent in a network can sense only the relative bearings to their nearest neighbors. The study of this topic is motivated mainly by the rapid development of bearing-only sensors, such as optical cameras and sensor arrays. This article provides a tutorial review on this topic, focusing on the problems of formation control and network localization. A key component of this review is a presentation of the recently developed *bearing rigidity theory*, which defines a necessary architectural feature of multiagent systems aiming to solve these two problems. This article presents a high-level summary of recently developed algorithms solving these problems, various simulation examples, and discussions pointing to the relevant literature and important remaining challenges in this area.

the stiffness or flexibility of structures formed by rigid bodies connected by flexible linkages or hinges. The study of distance rigidity has a long history as a formal mathematical discipline [29]–[36]. In recent years, it has played a fundamental role in distance-based formation control [37]–[45] and distance-based network localization [4], [5], [46]. One goal of this article is to compare the distance and bearing rigidity theories by highlighting their similarities and differences.

This article addresses three important applications of the bearing rigidity theory in the area of the distributed control and estimation of multiagent systems, briefly described as follows.

- » *Bearing-based network localization*: Consider a network of stationary nodes where only a subset of the nodes know their own absolute positions. These special nodes are referred to as *anchors* while the others are *followers*. Suppose each follower node is able to measure the relative bearings of its neighbors and share the estimates of its own position with its neighbors by wireless communication. The aim of bearing-based network localization is to localize the follower nodes using the bearing measurements and the anchors' absolute positions [6], [47]–[52]. Here, the network localization problem may also be called network self-localization, which is usually the first step for a sensor network to provide other services, such as positioning or monitoring. Network localization is essential for sensor networks in environments where GPS signals are not available, reliable, or sufficiently accurate.
- » *Bearing-based formation control*: Consider a group of mobile agents where each agent is able to obtain the relative positions of its neighbors. The aim of bearing-based formation control is to steer the agents from some initial spatial configuration to a target formation with a desired geometric pattern predefined by interneighbor bearings [24], [53]–[56]. Since the target formation is invariant in

terms of scaling variations, bearing-based formation control provides a simple solution for formation scale control, which is a practically useful technique to adjust the scale of a formation so that the agents can dynamically respond to the environment to achieve, for example, obstacle avoidance, such as passing through narrow passages [57], [58]. Note that the bearing-based formation control problem is dual with respect to the bearing-based network localization problem. When the agent dynamics are modeled as single integrators and the leaders are stationary, the two problems are indeed identical. However, this article also considers a broader range of cases in the formation control problem, namely, formation maneuvering using leaders and different models for the agent dynamics, including double integrators and unicycles.

- » *Bearing-only formation control*: The aim of bearing-only formation control is to steer a group of mobile agents to form a desired geometric pattern predefined by interneighbor bearings. Unlike bearing-based formation control, bearing-only formation control requires each agent only to measure the relative bearings of its neighbors, whereas relative positions are not required to be measured or estimated [10], [25], [59]–[65]. Bearing-only formation control provides a novel framework for implementing vision-based formation control tasks, where vision may be modeled as a bearing-only sensing approach. It also suggests that distance information may be redundant for achieving certain formation control tasks.

The notations for the networks and formations used throughout this article are given in “Notation for Networks and Formations.”

## BEARING RIGIDITY THEORY

Bearing rigidity theory studies the conditions where the geometric pattern of a network can be uniquely determined if the

### Notation for Networks and Formations

Given a network of  $n$  nodes in  $\mathbb{R}^d$ , where  $n \geq 2, d \geq 2$ , let the position of node  $i$  be  $p_i \in \mathbb{R}^d$  and the configuration of the points be  $p = [p_1^T, \dots, p_n^T]^T \in \mathbb{R}^{dn}$ . The interaction among the nodes is described by a graph  $\mathcal{G} = (\mathcal{V}, \mathcal{E})$  that consists of a vertex set  $\mathcal{V} = \{1, \dots, n\}$  and an edge set  $\mathcal{E} \subseteq \mathcal{V} \times \mathcal{V}$ . If  $(i, j) \in \mathcal{E}$ , then node  $i$  receives information from node  $j$ , and node  $j$  is adjacent to  $i$ . The set of neighbors of vertex  $i$  is denoted as  $\mathcal{N}_i = \{j \in \mathcal{V} : (i, j) \in \mathcal{E}\}$ . This article focuses on undirected graphs, where  $(i, j) \in \mathcal{E} \Leftrightarrow (j, i) \in \mathcal{E}$ .

Let  $m$  be the number of undirected edges in the graph. An orientation of an undirected graph is the assignment of a direction to each edge. An oriented graph is an undirected graph together with an orientation. The incidence matrix  $H \in \mathbb{R}^{m \times n}$  of an oriented graph is the  $\{0, \pm 1\}$  matrix, with rows indexed by edges and columns by vertices.

A network, denoted as  $(\mathcal{G}, p)$ , is  $\mathcal{G}$  with its vertex  $i \in \mathcal{V}$  mapped to  $p_i$ . A network may be called a *formation* in the context of formation control. For a network  $(\mathcal{G}, p)$ , define the edge and bearing vectors for  $(i, j) \in \mathcal{E}$  as  $e_{ij} = p_j - p_i$  and  $g_{ij} = e_{ij} / \|e_{ij}\|$ , respectively. Here  $g_{ij}$  is the unit vector pointing from  $p_i$  to  $p_j$  that represents the relative bearing of  $p_i$  with respect to  $p_j$ . Note that  $e_{ij} = -e_{ji}$  and  $g_{ij} = -g_{ji}$ . Consider an orientation of the graph  $\mathcal{G}$  and suppose  $(i, j)$  corresponds to the  $k$ th edge in the oriented graph. Then the edge and bearing vectors may be expressed as  $e_k = p_j - p_i$  and  $g_k = e_k / \|e_k\|$ , where  $k \in \{1, \dots, m\}$ . Let  $e = [e_1^T, \dots, e_m^T]^T$  and  $g = [g_1^T, \dots, g_m^T]^T$ . Note that  $e = (H \otimes I_d)p$ , where  $\otimes$  denotes the Kronecker product. In this article,  $\text{Null}(\cdot)$  and  $\text{Range}(\cdot)$  denote the null and range spaces of a matrix, respectively. Denote  $\mathbf{1}_n \triangleq [1, \dots, 1]^T \in \mathbb{R}^n$ . Let  $\|\cdot\|$  be the Euclidean norm of a vector or the spectral norm of a matrix and  $I_d \in \mathbb{R}^{d \times d}$  the identity matrix.

bearing of each edge in the network is fixed. Equivalently stated, bearing rigidity studies the conditions where two networks have the same geometric pattern if they have the same bearings. To illustrate this idea, the two networks in Figure 1(a) have the same bearings but different geometric patterns. As a result, they are not bearing rigid. The two networks in Figure 1(b) have the same bearings and geometric pattern (modulo a scaling and translational factor). The two networks can be shown to be bearing rigid, and the rigorous proof of this result relies on the theory presented in this section.

There are three different notions of bearing rigidity: bearing, global bearing, and infinitesimal bearing. The first two are not of practical interest because they cannot ensure unique geometric patterns of networks. The third, infinitesimal bearing rigidity, is the most important. Its properties are discussed in detail in this section. The precise definitions of the three types of bearing rigidity are given in “Key Definitions in Bearing Rigidity Theory.” These definitions are analogous to those in the distance rigidity theory, which are listed in “Key Definitions in Distance Rigidity Theory” for the purpose of comparison. It is worth noting that an orthogonal projection matrix plays a key role in bearing rigidity theory. The properties of the projection matrix are summarized in “An Orthogonal Projection Matrix.” Moreover, a bearing (which is represented by a unit vector) must be expressed in a specific reference frame. In this article, the bearings in a network are all expressed in a common reference frame.

### Properties of Infinitesimal Bearing Rigidity

Infinitesimal bearing rigidity has two key properties. The first is a geometric property [28, Th. 6], namely, that the positions of the nodes in a network can be uniquely determined up to a translational and scaling factor by the bearings if and only if the network is infinitesimally bearing rigid. The second is an algebraic property [28, Th. 4]: a network is infinitesimally bearing rigid in the  $d$ -dimensional space if and only if the bearing rigidity matrix  $R_B$  satisfies

$$\text{Null}(R_B) = \text{span}\{\mathbf{1}_n \otimes I_d, p\}, \quad (1)$$

or, equivalently,

$$\text{rank}(R_B) = dn - d - 1. \quad (2)$$

The definition of the bearing rigidity matrix  $R_B$  is given in “Key Definitions in Bearing Rigidity Theory.” Because of the aforementioned two properties, infinitesimal bearing rigidity not only ensures the unique geometric pattern of a network but can be conveniently examined by a mathematical condition. Examples of infinitesimally bearing-rigid networks are given in Figure 2.

The notion of infinitesimal bearing rigidity is defined based on the bearing rigidity matrix. The term *infinitesimal* is due to the fact that the bearing rigidity matrix is the first-order derivative (the Jacobian) of the bearing vectors with

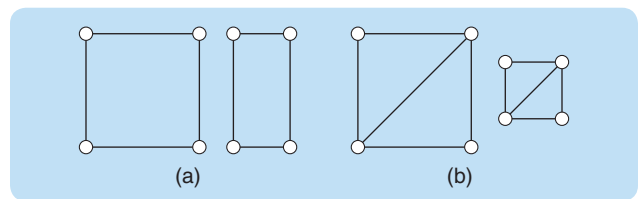


**FIGURE 1** An illustration of bearing rigidity. (a) The networks are not bearing rigid because the same interneighbor bearings may lead to different geometric patterns of the networks (for example, a square on the left and a rectangle on the right). (b) The networks are bearing rigid because the same interneighbor bearings imply the same geometric pattern, although the networks may differ in terms of translation and scale.

respect to the positions of the nodes. It must be noted that infinitesimal bearing rigidity is a global property in the sense that the bearings can uniquely determine the geometric pattern of a network. The term infinitesimal may be removed in this article when the context is clear.

An infinitesimal bearing motion of a network is a motion of some nodes that preserves all of the bearings. All of the infinitesimal bearing motions of a network form the null space of the bearing rigidity matrix. There are two types of trivial infinitesimal bearing motions: the translational and scaling motions of the entire network. These two types of trivial motions correspond to the vectors in  $\text{span}\{\mathbf{1}_n \otimes I_d, p\}$ . As a result, the rank condition in (1) means that a network is infinitesimally bearing rigid if and only if all of the infinitesimal bearing motions are trivial. This provides an intuitive way to examine bearing rigidity. For example, the networks in Figure 3 are not bearing rigid because they have nontrivial infinitesimal bearing motions.

An alternative necessary and sufficient condition for infinitesimal bearing rigidity is based on a special matrix termed the *bearing Laplacian* [66]. The bearing Laplacian of a network can be viewed as a weighted graph Laplacian matrix with weights that are matrices [67]; thus, the bearing Laplacian describes not only the topological structure of the network but the values of the edge bearings. The definition and properties of the bearing Laplacian are summarized in “Bearing Laplacian of Networks.” For a network with an undirected graph, the bearing Laplacian has the same rank and null space as the bearing rigidity matrix [66, Lemma 2]. It then follows from (1) and (2) that a network is infinitesimally bearing rigid if and only if

$$\text{Null}(\mathcal{B}) = \text{span}\{\mathbf{1}_n \otimes I_d, p\}, \quad (3)$$

or, equivalently,

$$\text{rank}(\mathcal{B}) = dn - d - 1. \quad (4)$$

Compared to the bearing rigidity matrix, the bearing Laplacian is more convenient to use because it is symmetric and positive semidefinite for undirected graphs. When the underlying graph is directed, the bearing Laplacian and the

## Key Definitions in Bearing Rigidity Theory

### DEFINITION S1 (BEARING EQUIVALENCY)

Two networks  $(\mathcal{G}, p)$  and  $(\mathcal{G}, p')$  are *bearing equivalent* if  $P_{(p_i-p_j)}(p'_i-p'_j) = 0$  for all  $(i, j) \in \mathcal{E}$ .

### DEFINITION S2 (BEARING CONGRUENCY)

Two networks  $(\mathcal{G}, p)$  and  $(\mathcal{G}, p')$  are *bearing congruent* if  $P_{(p_i-p_j)}(p'_i-p'_j) = 0$  for all  $i, j \in \mathcal{V}$ .

### DEFINITION S3 (BEARING RIGIDITY)

A network  $(\mathcal{G}, p)$  is *bearing rigid* if there exists a constant  $\epsilon > 0$  such that any network  $(\mathcal{G}, p')$  that is bearing equivalent to  $(\mathcal{G}, p)$  and satisfies  $\|p' - p\| < \epsilon$  is also bearing congruent to  $(\mathcal{G}, p)$ .

### DEFINITION S4 (GLOBAL BEARING RIGIDITY)

A network  $(\mathcal{G}, p)$  is *globally bearing rigid* if an arbitrary network that is bearing equivalent to  $(\mathcal{G}, p)$  is also bearing congruent to  $(\mathcal{G}, p)$ .

Consider an oriented graph where the interneighbor bearings can be expressed by  $\{g_k\}_{k=1}^m$ . Define the bearing function  $F_B: \mathbb{R}^{dn} \rightarrow \mathbb{R}^{dm}$  as

$$F_B(p) = [g_1^T, \dots, g_m^T]^T \in \mathbb{R}^{dm}.$$

The *bearing rigidity matrix* is defined as the Jacobian of the bearing function

$$R_B(p) = \frac{\partial F_B(p)}{\partial p} \in \mathbb{R}^{dm \times dn}. \quad (\text{S1})$$

A matrix-vector form  $R_B(p)$  is

$$R_B(p) = \text{diag}(P_{g_1}/\|e_1\|, \dots, P_{g_m}/\|e_m\|)(H \otimes I_d).$$

Let  $\delta p \in \mathbb{R}^{dn}$  be a variation of the configuration  $p$ . If  $R_B(p)\delta p = 0$ , then  $\delta p$  is an *infinitesimal bearing motion* of  $(\mathcal{G}, p)$ . An infinitesimal bearing motion is *trivial* if it corresponds only to a translation and a scaling of the entire network.

### DEFINITION S5 (INFINITESIMAL BEARING RIGIDITY)

A network is *infinitesimally bearing rigid* if all the infinitesimal bearing motions are trivial.

The relation between bearing rigidity, global bearing rigidity, and infinitesimal bearing rigidity is illustrated in Figure S1. Details of these notions can be found in [28].

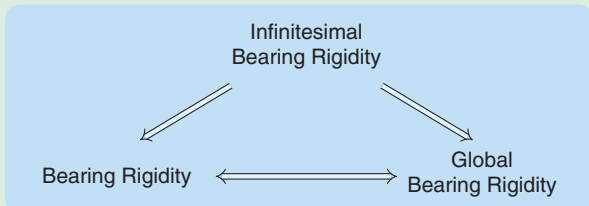


**FIGURE S1** The relation between bearing rigidity, global bearing rigidity, and infinitesimal bearing rigidity. Infinitesimal bearing rigidity implies both bearing rigidity and global bearing rigidity. Global bearing rigidity and bearing rigidity imply each other.

## Key Definitions in Distance Rigidity Theory

### DEFINITION S6 (DISTANCE EQUIVALENCY)

Two networks  $(\mathcal{G}, p)$  and  $(\mathcal{G}, p')$  are *distance equivalent* if  $\|p_i - p_j\| = \|p'_i - p'_j\|$  for all  $(i, j) \in \mathcal{E}$ .

### DEFINITION S7 (DISTANCE CONGRUENCY)

Two networks  $(\mathcal{G}, p)$  and  $(\mathcal{G}, p')$  are *distance congruent* if  $\|p_i - p_j\| = \|p'_i - p'_j\|$  for all  $i, j \in \mathcal{V}$ .

### DEFINITION S8 (DISTANCE RIGIDITY)

A network  $(\mathcal{G}, p)$  is *distance rigid* if there exists a constant  $\epsilon > 0$  such that any network  $(\mathcal{G}, p')$  that is distance equivalent to  $(\mathcal{G}, p)$  and satisfies  $\|p' - p\| < \epsilon$  is also distance congruent to  $(\mathcal{G}, p)$ .

### DEFINITION S9 (GLOBAL DISTANCE RIGIDITY)

A network  $(\mathcal{G}, p)$  is *globally distance rigid* if an arbitrary network that is distance equivalent to  $(\mathcal{G}, p)$  is also distance congruent to it.

Consider an oriented graph, where the interneighbor distances can be expressed by  $\{d_k\}_{k=1}^m$ . Define the distance function  $F_D: \mathbb{R}^{dn} \rightarrow \mathbb{R}^{dm}$  as

$$F_D(p) = [\|e_1\|^2, \dots, \|e_m\|^2]^T / 2 \in \mathbb{R}^m.$$

The *distance rigidity matrix* is defined as the Jacobian of the distance function

$$R_D(p) = \frac{\partial F_D(p)}{\partial p} \in \mathbb{R}^{m \times dn}. \quad (\text{S2})$$

A matrix-vector form  $R_D(p)$  is

$$R_D(p) = \text{diag}(e_1^T, \dots, e_m^T)(H \otimes I_d).$$

Let  $\delta p \in \mathbb{R}^{dn}$  be a variation of the configuration  $p$ . If  $R_D(p)\delta p = 0$ , then  $\delta p$  is an *infinitesimal distance motion* of  $(\mathcal{G}, p)$ . An infinitesimal distance motion is *trivial* if it corresponds only to a translation and a rotation of the entire network.

### DEFINITION S10 (INFINITESIMAL DISTANCE RIGIDITY)

A network is *infinitesimally distance rigid* if all of the infinitesimal distance motions are trivial.

The relation between distance rigidity, global distance rigidity, and infinitesimal distance rigidity is illustrated in Figure S2. Details of these notions can be found in [29]–[32] and [36].

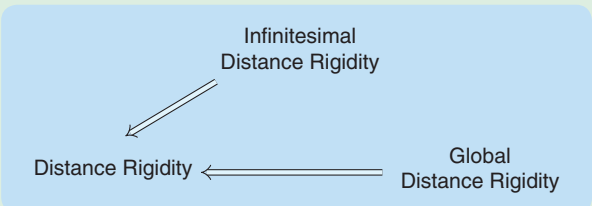


**FIGURE S2** The relation between distance rigidity, global distance rigidity, and infinitesimal distance rigidity. Both infinitesimal and global distance rigidity imply distance rigidity. Infinitesimal and global distance rigidity do not imply each other.

bearing rigidity matrix may have different ranks and null spaces [68, Th. 4].

### Construction of Infinitesimally Bearing-Rigid Networks

The previous discussion provided an overview of the properties defining a bearing-rigid network. It is also of interest to explore how to construct a bearing-rigid network by adding well-placed edges and nodes in a network. Although a network is jointly characterized by its underlying graph and the configuration of the nodes, the infinitesimal bearing rigidity of a network is primarily determined by the

underlying graph rather than its configuration [69, Lemma 2]. Given a graph, if there exists at least one configuration such that the network is infinitesimally bearing rigid, then for almost all configurations, the corresponding networks are infinitesimally bearing rigid. Such graphs are called *generically bearing rigid* [69]. If a graph is not generically bearing rigid, then the corresponding network is not infinitesimally bearing rigid for any configurations. As a result, constructing infinitesimally bearing-rigid networks requires the construction of generically bearing-rigid graphs.

One of the best-known methods for rigid graph construction is the Henneberg construction, originally proposed for

### An Orthogonal Projection Matrix

For any nonzero vector  $x \in \mathbb{R}^d$  ( $d \geq 2$ ), define an orthogonal projection matrix as

$$P(x) = I_d - \frac{x \cdot x^T}{\|x\|^2} \in \mathbb{R}^{d \times d}.$$

For notational simplicity, denote  $P_x = P(x)$ . The matrix  $P_x$  is an orthogonal projection matrix that geometrically projects any vector onto the orthogonal complement of  $x$  (see Figure S3).

Matrix  $P_x$  satisfies  $P_x^T = P_x$ ,  $P_x^2 = P_x$ , and  $\text{Null}(P_x) = \text{span}\{x\}$ . This matrix is positive semidefinite, with one eigenvalue equal to zero and  $d - 1$  eigenvalues equal to one. Other properties of  $P_x$  are summarized as follows.

- Any two nonzero vectors  $x, y \in \mathbb{R}^d$  are parallel if and only if  $P_x y = 0$  [28, Lemma 1].
- Any two unit vectors  $x, y \in \mathbb{R}^d$  satisfy  $x^T P_x y = y^T P_x x$  [28, Lemma 8].
- For any nonzero vectors  $x_1, \dots, x_m \in \mathbb{R}^d$  where  $m \geq 2$ ,  $d \geq 2$ , the matrix  $\sum_{i=1}^m P_{x_i} \in \mathbb{R}^{d \times d}$  is nonsingular if and only if at least two of  $x_1, \dots, x_m$  are not collinear [69, Lemma 3].
- For any nonzero vector  $x \in \mathbb{R}^2$ , denote  $x^\perp \in \mathbb{R}^2$  as a nonzero normal vector that satisfies  $x^T x^\perp = 0$ . Then,  $P_x = x^\perp (x^\perp)^T / \|x^\perp\|^2$ . The proof follows from the fact that the matrix  $A = [x/\|x\|, x^\perp/\|x^\perp\|] \in \mathbb{R}^{2 \times 2}$  satisfies  $A^T A = A A^T = I_2$ .
- For any two nonzero vectors  $x, y \in \mathbb{R}^d$ , if  $\theta \in [0, \pi]$  is the angle between them so that  $x^T y = \|x\| \|y\| \cos \theta$ , then

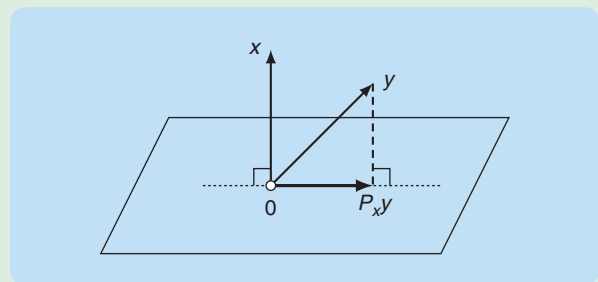


**FIGURE S3** An illustration of the orthogonal projection matrix. Given any nonzero  $x, y \in \mathbb{R}^d$ , the vector  $P_x y$  is the orthogonal projection of  $y$  onto the orthogonal complement of  $x$ .

$\|P_x - P_y\| = \sin \theta$  [66, Lemma 5]. This property has been used to analyze the perturbation of the orthogonal projection matrix.

- If  $x \in \mathbb{R}^3$  is a unit vector, then  $P_x = -[x]_x^2$ , where

$$[x]_x = \begin{bmatrix} 0 & -x_3 & x_2 \\ x_3 & 0 & -x_1 \\ -x_2 & x_1 & 0 \end{bmatrix} \in \mathbb{R}^{3 \times 3}$$

is the skew-symmetric matrix associated with  $x$  [7, Th. 2.11]. This property has been used in [72, eq. (6)].

The orthogonal projection matrix plays an important role in bearing rigidity theory and its applications.

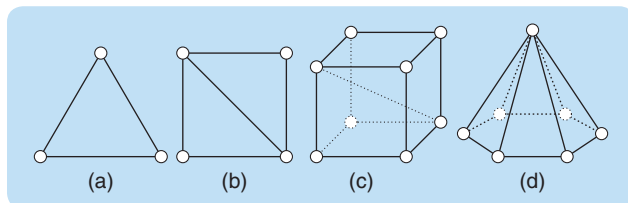


**FIGURE 2** Examples of infinitesimally bearing-rigid networks: the networks in (a) and (b) are 2D and the networks in (c) and (d) are 3D. It can be verified that each of these networks satisfies  $\text{rank}(R_B) = dn - d - 1$ . The networks in (a), (b), and (c) also satisfy the Laman condition and can, therefore, be generated using a Henneberg construction. Note that the two networks in (c) and (d) are infinitesimally bearing rigid but not infinitesimally distance rigid.

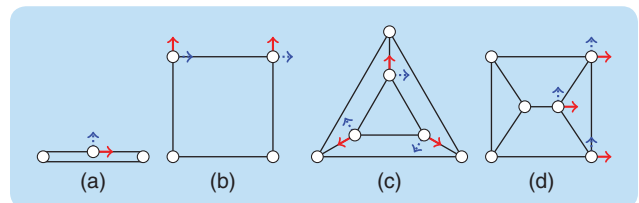


**FIGURE 3** Examples of noninfinitesimally bearing-rigid networks. The red/solid arrows represent nontrivial infinitesimal bearing motions that preserve all of the interneighbor bearings. These networks also are not infinitesimally distance rigid because they have nontrivial infinitesimal distance motions (see the blue/dotted arrows). Note that the infinitesimal distance motions are perpendicular to the infinitesimal bearing motions.

## Bearing Laplacian of Networks

Given the network  $(\mathcal{G}, p)$  with no collocated nodes, define the bearing Laplacian  $\mathcal{B} \in \mathbb{R}^{dn \times dn}$  as [66]

$$[\mathcal{B}]_{ij} = \begin{cases} 0_{d \times d}, & i \neq j, (i, j) \notin \mathcal{E}, \\ -P_{g_{ij}}, & i \neq j, (i, j) \in \mathcal{E}, \\ \sum_{k \in \mathcal{N}_i} P_{g_{ik}}, & i = j, i \in \mathcal{V}, \end{cases}$$

where  $[\mathcal{B}]_{ij} \in \mathbb{R}^{d \times d}$  is the  $ij$ th block of submatrix of  $\mathcal{B}$ . The bearing Laplacian can be viewed as a matrix-weighted Laplacian, which describes both the underlying graph and the interneighbor bearings of the network. See Figure S4 for an illustration.

For undirected graphs, the bearing Laplacian has the following properties [66, Lemma 2]:

- $\mathcal{B}$  is symmetric and positive semidefinite because, for any  $x = [x_1^T, \dots, x_n^T]^T \in \mathbb{R}^{dn}$ ,

$$x^T \mathcal{B} x = \frac{1}{2} \sum_{i \in \mathcal{V}} \sum_{j \in \mathcal{N}_i} (x_i - x_j)^T P_{g_{ij}} (x_i - x_j) \geq 0.$$

- $\text{rank}(\mathcal{B}) \leq dn - d - 1$  and  $\text{span}\{\mathbf{1} \otimes I_d, p\} \subseteq \text{Null}(\mathcal{B})$  for any network.
- $\text{rank}(\mathcal{B}) = dn - d - 1$  and  $\text{Null}(\mathcal{B}) = \text{span}\{\mathbf{1} \otimes I_d, p\}$  if and only if the network is infinitesimally bearing rigid.

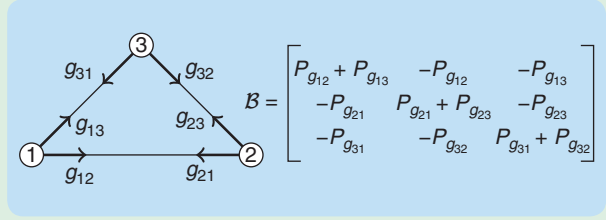


**FIGURE S4** An example to demonstrate bearing Laplacian. The network is the complete graph on three nodes. The bearing Laplacian has the same structure as a weighted graph Laplacian matrix [67], with the weights on each edge corresponding to the projection matrices  $P_{g_{ij}}$ .

In a network with  $n_a$  anchors and  $n_f = n - n_a$  followers, the bearing Laplacian may be partitioned into

$$\mathcal{B} = \begin{bmatrix} \mathcal{B}_{aa} & \mathcal{B}_{af} \\ \mathcal{B}_{fa} & \mathcal{B}_{ff} \end{bmatrix},$$

where  $\mathcal{B}_{ff} \in \mathbb{R}^{dn_f \times dn_f}$ . For any network,  $\mathcal{B}_{ff}$  is positive semidefinite and satisfies  $\mathcal{B}_{ff} p_f = -\mathcal{B}_{fa} p_a$  [66, Lemma 3]. In the context of formation control, the anchors are called leaders and the subscript  $a$  is replaced by  $\ell$ .

the distance rigidity theory [34]. A Henneberg construction starting from an edge connecting two vertices results in a Laman graph [70]. For a tutorial on Laman graphs and Henneberg construction, see “Laman Graphs and Henneberg Construction.”

In bearing rigidity theory, all Laman graphs are generically bearing rigid in arbitrary dimensions [69, Th. 1]. That means if the underlying graph of a network is Laman, then the network is infinitesimally bearing rigid for almost all configurations in an arbitrary dimension. Figure 4 illustrates the Henneberg construction procedure for a 3D infinitesimally bearing-rigid network whose underlying graph is Laman. Note that the Laman condition is merely sufficient but not necessary for generic bearing rigidity. A counterexample is given in Figure 5, where the graph is generically bearing rigid but not Laman. However, for networks in the plane, a graph is generically bearing rigid if and only if it is Laman [69, Th. 2].

Since a Laman graph has  $2n - 3$  edges, where  $n$  is the number of nodes,  $2n - 3$  edges are sufficient to guarantee the bearing rigidity of a network in an arbitrary dimension. For example, every network in Figure 4 is bearing rigid in the 3D space and has  $2n - 3$  edges. It must be noted that  $2n - 3$  is not the minimum number of edges required to ensure bearing rigidity. The counterexample given in Figure 5 shows that a graph with fewer than  $2n - 3$  edges may be generically bearing rigid in three dimensions. It is still an open problem to construct all

generically bearing-rigid graphs. A comparison between the bearing and distance rigidity theories is given in “Comparison of Bearing Rigidity and Distance Rigidity.”

## BEARING-BASED NETWORK LOCALIZATION

This section introduces the theory of bearing-based network localization that addresses two fundamental problems. The first is *localizability*, which describes whether or not a network can be localized. The second problem is *how* to localize a network in a distributed manner if it is localizable.

Consider a network of nodes where the first  $n_a$  nodes are anchors and the remaining  $n_f$  ( $n_f = n - n_a$ ) nodes are followers. Let  $\mathcal{V}_a = \{1, \dots, n_a\}$  and  $\mathcal{V}_f = \mathcal{V} \setminus \mathcal{V}_a$  be the sets of anchors and followers, respectively. The true positions of the leaders and followers are denoted as  $p_a = [p_1^T, \dots, p_{n_a}^T]^T$  and  $p_f = [p_{n_a+1}^T, \dots, p_n^T]^T$ , respectively. The aim of network localization is to determine the positions of the followers  $\{p_i\}_{i \in \mathcal{V}_f}$  using the edge bearings  $\{g_{ij}\}_{(i,j) \in \mathcal{E}}$  and the positions of the anchors  $\{p_i\}_{i \in \mathcal{V}_a}$ . All interneighbor bearings are expressed in a common reference frame.

### Bearing-Based Localizability

Localizing the follower nodes solves for  $\hat{p}_i$ , the estimate of  $p_i$  for all  $i \in \mathcal{V}_f$ , obtained from the set of nonlinear equations

$$\begin{cases} \hat{p}_j - \hat{p}_i = g_{ij}, & (i, j) \in \mathcal{E}, \\ \|\hat{p}_j - \hat{p}_i\| = g_{ij}, & (i, j) \in \mathcal{E}, \\ \hat{p}_i = p_i, & i \in \mathcal{V}_a. \end{cases} \quad (5)$$

## Laman Graphs and Henneberg Construction

An undirected graph  $\mathcal{G} = (\mathcal{V}, \mathcal{E})$  is called *Laman* if  $m = 2n - 3$ , and every subset of  $k \geq 2$  vertices spans at most  $2k - 3$  edges [70]. Laman graphs can be characterized by the Henneberg construction, as described below. Given a graph  $\mathcal{G} = (\mathcal{V}, \mathcal{E})$ , a new graph  $\mathcal{G}' = (\mathcal{V}', \mathcal{E}')$  is formed by adding a new vertex  $v$  to  $\mathcal{G}$  and performing one of the following two operations:

- 1) **Vertex addition:** Connect vertex  $v$  to any two existing vertices  $i, j \in \mathcal{V}$ . In this case,  $\mathcal{V}' = \mathcal{V} \cup \{v\}$  and  $\mathcal{E}' = \mathcal{E} \cup \{(v, i), (v, j)\}$ . See Figure S5(a) for an illustration.
- 2) **Edge splitting:** Consider three vertices  $i, j, k \in \mathcal{V}$  with  $(i, j) \in \mathcal{E}$ . Connect vertex  $v$  to  $i, j, k$ , and delete  $(i, j)$ . In this case,  $\mathcal{V}' = \mathcal{V} \cup \{v\}$  and  $\mathcal{E}' = \mathcal{E} \cup \{(v, i), (v, j), (v, k)\} \setminus \{(i, j)\}$ . See Figure S5(b) for a depiction.

A Henneberg construction starting from an edge connecting two vertices leads to a Laman graph [34]–[36]. The converse is also true. That is, if a graph is Laman, then it can be generated by a Henneberg construction [35, Lemma 2]. The underlying graphs of the networks

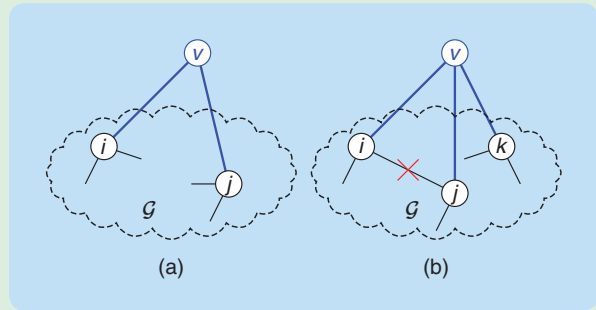


**FIGURE S5** The two operations of the Henneberg construction. The Henneberg construction can be used to generate all minimally infinitesimally distance-rigid graphs in the plane. The main goal is to ensure that (a) the vertex-addition operation and (b) the edge-splitting operation satisfy the Laman condition at each step.

in Figure 2(a)–(c) are Laman. Laman graphs play critical roles in the construction of distance-rigid and bearing-rigid networks.

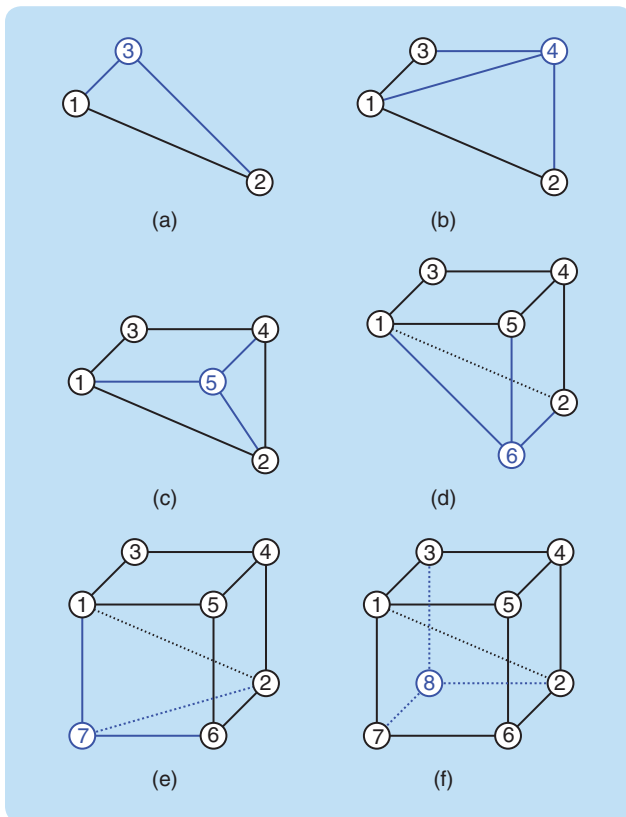


**FIGURE 4** An illustration of the Henneberg construction procedure. The Henneberg construction consists of two basic operations: vertex addition and edge splitting. In this example, the procedure is used to generate an infinitesimally bearing-rigid network in a 3D ambient space. At each step, the underlying graph of the network is Laman. Step (a): vertex addition; steps (b)–(f): edge splitting.

The true location  $p$  of the network is a feasible solution to (5). However, there may exist an infinite number of other feasible solutions. This leads to the definition of localizability. A network  $(\mathcal{G}, p)$  is *bearing localizable* if the true position  $p$  is the unique feasible solution to (5). It can be further shown that  $p$  is the unique solution to (5) if and only if  $p$  is the unique global minimizer of the least-squares problem [66, Lemma 1]

$$\min_{\hat{p} \in \mathbb{R}^{dn}} J(\hat{p}) = \frac{1}{2} \sum_{i \in \mathcal{V}} \sum_{j \in \mathcal{N}_i} \|P_{g_{ij}}(\hat{p}_i - \hat{p}_j)\|^2 = \hat{p}^T \mathcal{B} \hat{p}, \quad (6)$$

subject to  $\hat{p}_i = p_i$  for  $i \in \mathcal{V}_a$ . It has been proven that  $p$  is the unique minimizer of (6) if and only if the matrix  $\mathcal{B}_{ff}$

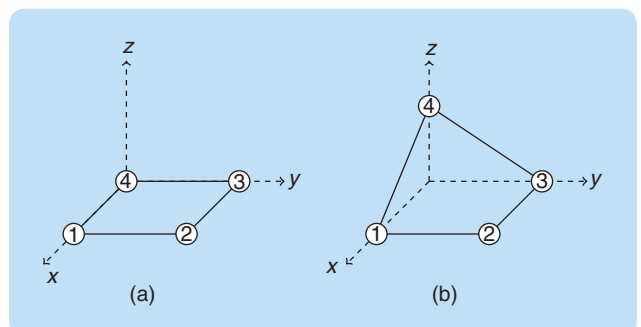


**FIGURE 5** An example of generically bearing rigid graphs that are not Laman. (a) The configuration is in the  $xy$  plane, and the network is not bearing rigid. (b) The configuration is 3D, and the network is bearing rigid. It can be verified that  $\text{rank}(\mathcal{B}) = dn - d - 1$  for (b).

## Comparison of Bearing Rigidity and Distance Rigidity

Both bearing and distance rigidity theories address the same problem of when the geometric pattern of a network can be uniquely determined. The difference is that the bearing rigidity theory considers interneighbor bearings, whereas the distance rigidity theory focuses on interneighbor distances. The term *unique pattern* in bearing rigidity theory means that the location of a network can be determined up to a translational and scaling factor, while in distance rigidity theory it signifies that the network can be determined up to a translational and rotational factor.

One connection between the two rigidity theories is that infinitesimal bearing rigidity is equivalent to infinitesimal distance rigidity in two dimensions [28, Th. 8]. That is, a network in the plane is infinitesimally bearing rigid if and only if it is infinitesimally distance rigid. This equivalence property explains why distance rigidity theory could be used to analyze the problems of bearing-based network localization or formation control in the literature [49], [51], [64]. It also suggests that the infinitesimal distance rigidity of a network can be examined by its infinitesimal bearing rigidity. For example, it may not be straightforward to see that the networks in Figure 3(c) and (d) are not infinitesimally distance rigid. However, it is intuitive to see that they are not infinitesimally bearing rigid because there exist nontrivial infinitesimal bearing motions. It must be noted that the equivalence cannot be generalized to three or higher dimensions. For example, the 3D networks shown in Figure 2(c)–(e) are infinitesimally bearing rigid but not infinitesimally distance rigid.

Compared to infinitesimal distance rigidity, infinitesimal bearing rigidity possesses interesting properties, as follows.

- Infinitesimal bearing rigidity not only ensures the unique pattern of a network but also can be easily examined by a rank condition. As a comparison, infinitesimal distance rigidity may not be able to ensure a unique pattern, although it can be examined by a rank condition.
- An infinitesimally bearing-rigid network remains infinitesimally bearing rigid when the dimension is lifted into a higher dimension [28, Th. 7]. As a comparison, a network that is infinitesimally distance rigid in the plane may be flexible in a higher dimension.
- In bearing rigidity theory, a Laman graph is generically bearing rigid in arbitrary dimensions, and at most  $2n - 3$  edges would be sufficient to guarantee the bearing rigidity of a network in an arbitrary dimension. As a comparison, although a Laman graph embedded in a generic configuration is infinitesimally distance rigid [30], [34]–[37], this result (known as Laman's theorem [70]) is valid merely in 2D spaces. In three or higher dimensions, extra conditions and more edges are required to guarantee distance rigidity.

This comparison is summarized in Table S1.

Why bearing rigidity has appealing properties in high dimensions can be explained from the perspective of degree of freedom. For example, consider a network of  $n$  nodes in the  $d$ -dimensional space. The network has  $dn$  degrees of freedom. To ensure the

is nonsingular [66, Th. 1]. The definition of  $\mathcal{B}_{ff}$  is given in "Bearing Laplacian of Networks." When  $\mathcal{B}_{ff}$  is nonsingular, the positions of the followers can be solved as  $\hat{p}_f^* = -\mathcal{B}_{ff}^{-1} \mathcal{B}_{fa} p_a$ . Examples of bearing-localizable and nonlocalizable networks are given in Figures 6 and 7, respectively.

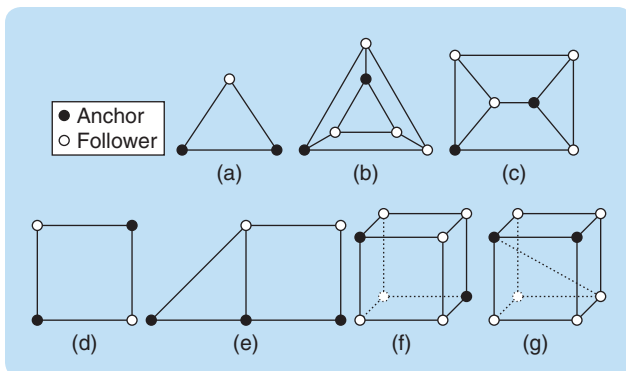


**FIGURE 6** Examples of bearing-localizable networks. The networks are localizable because  $\mathcal{B}_{ff}$  of each network is nonsingular. The intuitive interpretation is that every infinitesimal bearing motion involves at least one anchor. Note that the networks in (b)–(f) are not infinitesimally bearing rigid but are localizable.

While the nonsingularity of  $\mathcal{B}_{ff}$  is an algebraic condition for bearing localizability, it does not provide any suggestion as to what a bearing-localizable network looks like. The following conditions can provide more insight into bearing-localizable networks. First, a necessary and sufficient rigidity condition for bearing localizability is that every infinitesimal bearing motion of a network must involve at least one anchor [66, Th. 2]. Specifically, if there exists a nonzero infinitesimal bearing motion for a network, then there would exist different networks having exactly the same bearings as the true network. As a result, infinitesimal bearing motions introduce ambiguities in

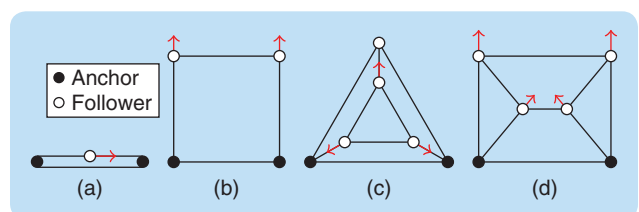


**FIGURE 7** Examples of networks that are not bearing localizable. The networks are not localizable because  $\mathcal{B}_{ff}$  of each network is singular. The intuitive interpretation is that the networks have infinitesimal bearing motions that correspond only to the followers (see the red arrows).

**TABLE S1 A comparison of infinitesimal bearing rigidity and infinitesimal distance rigidity.**

|                                 | <b>Infinitesimal Bearing Rigidity (IBR)</b>  | <b>Infinitesimal Distance Rigidity (IDR)</b>  |
|---------------------------------|--|---|
| <b>Unique geometric pattern</b> | Yes, IBR ensures the unique pattern of a network.  | No, IDR does not ensure the unique pattern of a network (global distance rigidity does).  |
| <b>Rank condition</b>           | Yes, IBR corresponds to a rank condition of the bearing rigidity matrix.   | Yes, IDR corresponds to a rank condition of the distance rigidity matrix.   |
| <b>Invariance to dimension</b>  | Yes, a network that is IBR in a lower dimension remains IBR in a higher dimension.   | No, a network that is IDR in a lower dimension may be flexible in a higher dimension. Universal distance rigidity is invariant to dimensions.           |
| <b>Minimum edge number</b>      | In an arbitrary dimension, $2n - 3$ edges are sufficient to ensure IBR. Less than $2n - 3$ edges may also be sufficient to ensure IBR in three or higher dimensions. | In the plane, $2n - 3$ is the minimum number of edges to ensure IDR. More than $2n - 3$ edges are required to ensure IDR in three or higher dimensions. |
| <b>Laman graphs</b>             | In an arbitrary dimension, Laman graphs mapped to almost all configurations result in IBR networks.  | In the plane, Laman graphs mapped to almost all configurations result in IDR networks. A similar result does not exist in higher dimensions.            |

rigidity of the network, there must exist sufficient distance or bearing constraints to reduce the degrees of freedom of the network to certain desired values. Given a distance-rigid network, when lifted into a higher dimension, the network's degrees of freedom increase while the number of constraints posed by interneighbor distance remain the same. To preserve distance rigidity in higher dimensions, more distance constraints are required.

As a comparison, when lifted into a higher dimension, the number of independent constraints posed by interneighbor bearings also increases. For example, a bearing in the plane is equivalent to an azimuth angle, whereas a bearing in the 3D space is equivalent to two bearing angles: azimuth and altitude. As a result, the same number of bearings is still able to preserve the bearing rigidity of the network.

the localization of the true network. When the infinitesimal motion involves at least one anchor, the ambiguities can be resolved by the anchors whose positions are known, and hence the network location can be uniquely determined. This rigidity condition provides an intuitive way to examine network localizability (see, for example, Figure 7).

The following condition indicates how many anchors are required to guarantee bearing localizability. The number of anchors in a bearing-localizable network in  $\mathbb{R}^d$  must satisfy [66, Corollary 1]

$$n_a \geq \frac{\dim(\text{Null}(\mathcal{B}))}{d} \geq \frac{d+1}{d}. \quad (7)$$

Inequality (7) has two important implications. The first is that every bearing-localizable network must have at least *two* anchors because  $(d+1)/d > 1$ . The second is that more anchors are required when the *degree of bearing rigidity* of the network is weak. Here, the degree of bearing rigidity [characterized by  $\dim(\text{Null}(\mathcal{B}))$ ] is strongest if  $\dim(\text{Null}(\mathcal{B}))$  reaches the smallest value of  $d+1$  (when the network is infinitesimally bearing rigid) and weak if its value is greater than  $d+1$ .

The following two conditions explicitly address the relation between bearing localizability and bearing rigidity.

- 1) A sufficient condition for a network to be bearing localizable is that it is infinitesimally bearing rigid and has at least two anchors [66, Corollary 3]. If a network is infinitesimally bearing rigid, then it can be uniquely determined up to a translation and scaling factor. If there are at least two anchors, then the translational and scaling ambiguity can be eliminated by the anchors, and, thus, the entire network can be fully determined. It must be noted that infinitesimal bearing rigidity is merely sufficient but not necessary for bearing localizability. For example, the networks in Figure 6(b)–(f) are bearing localizable but not infinitesimally bearing rigid.
- 2) Let  $(\bar{\mathcal{G}}, p)$  be the augmented network of  $(\mathcal{G}, p)$ , which is obtained from  $(\mathcal{G}, p)$  by connecting each pair of anchors (see Figure 8 for an illustration). Then, another sufficient condition for bearing localizability is that network  $(\mathcal{G}, p)$  is bearing localizable if the augmented network  $(\bar{\mathcal{G}}, p)$  is infinitesimally bearing rigid and there are at least two anchors [66, Corollary 2]. This condition is more relaxed, as it does not require  $(\mathcal{G}, p)$  to be infinitesimally bearing rigid.

When there are more than two anchors, the infinitesimal bearing rigidity of  $(\overline{\mathcal{G}}, p)$  is merely sufficient but not necessary for the bearing localizability of  $(\mathcal{G}, p)$ . See Figure 6(f) for a counterexample where the network is bearing localizable but the augmented network is not infinitesimally bearing rigid. When there are exactly two anchors, the infinitesimal bearing rigidity of  $(\overline{\mathcal{G}}, p)$  is both necessary and sufficient for the bearing localizability of  $(\mathcal{G}, p)$  [66, Th. 3].

### Distributed Localization Protocols

If a network is bearing localizable, then it must be determined how to localize it in a distributed manner. Suppose each node has an initial guess of its own position as  $\hat{p}_i(0)$ . The objective is to design a distributed protocol to drive  $\hat{p}_i(t) \rightarrow p_i$  for all  $i \in \mathcal{V}_f$  as  $t \rightarrow \infty$ . This objective can be achieved by the protocol [66]

$$\dot{\hat{p}}_i(t) = - \sum_{j \in N_i} P_{g_{ij}}(\hat{p}_i(t) - \hat{p}_j(t)), \quad i \in \mathcal{V}_f, \quad (8)$$

where  $P_{g_{ij}} = I_d - g_{ij}g_{ij}^T$ . Protocol (8) is the gradient-descent protocol for the objective function in the least-squares problem (6). The geometric interpretation of this protocol is illustrated in Figure 9. The expression of (8) is similar to the well-known linear consensus protocols [19], [21]. The difference is that the weight for each edge in (8) is an orthogonal

projection matrix while, in the consensus protocols, the weight for each edge is a scalar. This important distinction leads to very different properties of the dynamical system. The unique structure of the projection matrix is the key feature that enables (8) to solve the bearing-based network localization problem.

The compact matrix form of (8) is

$$\dot{\hat{p}}_f(t) = -\mathcal{B}_{ff}\hat{p}_f(t) - \mathcal{B}_{fa}p_a,$$

where  $\mathcal{B}$  is the bearing Laplacian of the true network. This protocol can globally localize the network if and only if the network is bearing localizable (that is, if  $\mathcal{B}_{ff}$  is nonsingular) [66, Th. 4]. Figure 10 shows a simulation example to demonstrate (8). The impact of measurement noise on bearing-based network localization was discussed in [66].

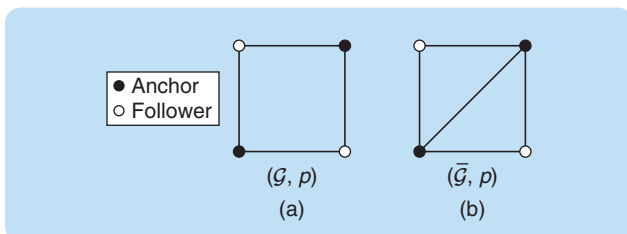


**FIGURE 8** An illustration of (a) a network  $(\mathcal{G}, p)$  and (b) its augmented network  $(\overline{\mathcal{G}}, p)$ . The augmented network is obtained from  $(\mathcal{G}, p)$  by connecting each pair of anchors in  $(\mathcal{G}, p)$ . Since deleting or adding the edge between any pair of anchors only changes  $\mathcal{B}_{aa}$  but not  $\mathcal{B}_{ff}$ ,  $(\mathcal{G}, p)$  and  $(\overline{\mathcal{G}}, p)$  have exactly the same  $\mathcal{B}_{ff}$ , and hence they have the same localizability properties.

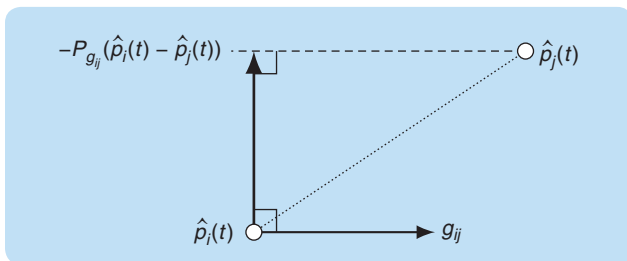


**FIGURE 9** The geometric interpretation of the bearing-based control law in (8). The term  $P_{g_{ij}}(\hat{p}_i(t) - \hat{p}_j(t))$  is perpendicular to  $g_{ij}$ , and it aims to steer agent  $i$  such that  $\hat{g}_{ij}(t)$  aligns with  $g_{ij}$ .

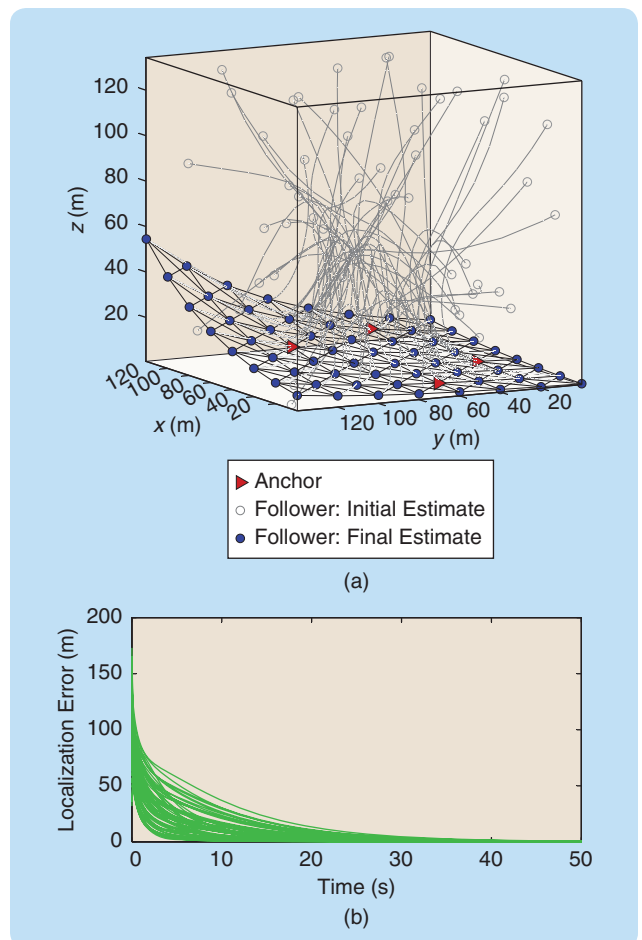


**FIGURE 10** A simulation example to demonstrate the localization protocol in (8): (a) the initial and final estimates and (b) the localization error  $\|\hat{p}_i(t) - p_i\|$ . The real network is located on a 3D surface. It consists of 210 edges and 64 nodes, four of which are anchors. The network is infinitesimally bearing rigid because  $\text{rank}(\mathcal{B}) = 188 = dn - d - 1$ . Therefore, the network is localizable, since there are more than two anchors. As can be seen, given a random initial guess, the localization error of each node converges to zero.

## BEARING-BASED FORMATION CONTROL

This section introduces the theory of bearing-based formation control, which studies how to steer a group of agents to achieve a bearing-constrained target formation using relative position measurements. Consider a group of mobile agents, where the first  $n_\ell$  agents are leaders and the remaining  $n_f$  ( $n_f = n - n_\ell$ ) agents are followers. Let  $\mathcal{V}_\ell = \{1, \dots, n_\ell\}$  and  $\mathcal{V}_f = \mathcal{V} \setminus \mathcal{V}_\ell$  be the sets of leaders and followers, respectively. The positions of the leaders and followers are denoted as  $p_\ell = [p_1^T, \dots, p_{n_\ell}^T]^T$  and  $p_f = [p_{n_\ell+1}^T, \dots, p_n^T]^T$ , respectively. The target formation is specified by the constant bearing constraints  $\{g_{ij}^*\}_{(i,j) \in \mathcal{E}}$  and the leader positions  $\{p_i(t)\}_{i \in \mathcal{V}_\ell}$ . The control objective is to govern the positions of the followers  $\{p_i(t)\}_{i \in \mathcal{V}_f}$  such that  $g_{ij}(t) \rightarrow g_{ij}^*$  as  $t \rightarrow \infty$  for all  $(i, j) \in \mathcal{E}$ . All of the bearings are expressed in a common reference frame.

### Bearing-Based Formation Control of Single Integrators

First, consider the case where the dynamics of each mobile agent can be modeled as the single integrator

$$\dot{p}_i(t) = u_i(t),$$

where  $u_i(t)$  is the velocity input to be designed. If the leaders are stationary, then the bearing-based formation control problem can be solved by [54]

$$\dot{p}_i(t) = - \sum_{j \in \mathcal{N}_i} P_{g_{ij}^*} (p_i(t) - p_j(t)), \quad i \in \mathcal{V}_f, \quad (9)$$

where  $P_{g_{ij}^*} = I_d - g_{ij}^* (g_{ij}^*)^T$ . The matrix form of the control law is

$$\dot{p}_f(t) = -\mathcal{B}_{ff} p_f(t) - \mathcal{B}_{f\ell} p_\ell,$$

where  $\mathcal{B}$  is the bearing Laplacian of the target formation. Control law (9) can globally stabilize a target formation if and only if the target formation is bearing localizable (that is, if  $\mathcal{B}_{ff}$  is nonsingular) [54]. Note that control law (9) has an expression similar to the network localization protocol in (8). In fact, the bearing-based formation control problem is mathematically equivalent to the bearing-based network localization problem when the target formation is stationary and each agent is a single integrator.

If the leaders move at a constant nonzero speed, then (9) would yield a constant nonzero tracking error. The tracking error may be eliminated using the following proportional-integral control law proposed in [71]

$$\dot{p}_i(t) = - \sum_{j \in \mathcal{N}_i} P_{g_{ij}^*} \left[ k_p (p_i(t) - p_j(t)) - k_I \int_0^t (p_i(\tau) - p_j(\tau)) d\tau \right], \quad (10)$$

where  $i \in \mathcal{V}_f$  and  $k_p$  and  $k_I$  are constant positive control gains. The target formation is globally stable under the action of control law (10) if and only if it is bearing localizable [71].

If the leader velocities are time varying, then (10) would fail to ensure zero tracking errors. The time-varying case can be handled by the following control law that requires velocity feedback:

$$\dot{p}_i(t) = -K_i^{-1} \sum_{j \in \mathcal{N}_i} P_{g_{ij}^*} [k_p (p_i(t) - p_j(t)) - \dot{p}_j(t)], \quad i \in \mathcal{V}_f, \quad (11)$$

where  $K_i = \sum_{j \in \mathcal{N}_i} P_{g_{ij}^*}$ . The stability of (11) is proven next. First, the nonsingularity of  $K_i$  is guaranteed by the bearing localizability of the target formation [55, Lemma 3]. Second, multiplying  $K_i$  on both sides of (11) yields  $\dot{\varepsilon}_i = -k_p \varepsilon_i$ , where  $\varepsilon_i = \sum_{j \in \mathcal{N}_i} P_{g_{ij}^*} (p_i(t) - p_j(t))$  for  $i \in \mathcal{V}_f$ . It follows that  $\varepsilon_i \rightarrow 0$  as  $t \rightarrow \infty$  for all  $i \in \mathcal{V}_f$ , and consequently  $g_{ij} \rightarrow g_{ij}^*$  when the network is bearing localizable.

Under the action of (10) and (11), the formation is able to perform translational and scaling formation maneuvers. A translational maneuver means that all agents move at a common velocity, such that the formation translates as a rigid body. A scaling maneuver means that the scale of the formation, which can be described by the distance from each agent to the formation centroid, varies while the geometric pattern of the formation is preserved. To achieve the scaling maneuver, the leaders need only to adjust the distances among them. One merit of the bearing-based control laws is that the desired maneuver is known only to the leaders, and the followers are not required to access or estimate it.

### Bearing-Based Formation Control of Double Integrators

Consider the case where the dynamics of each mobile agent can be modeled as a double integrator

$$\begin{aligned} \dot{p}_i(t) &= v_i(t), \\ \dot{v}_i(t) &= u_i(t), \end{aligned} \quad (12)$$

where  $u_i(t)$  is the acceleration input to be designed. If the velocities of the leaders are constant, then the bearing-based formation control problem can be solved by [55]

$$\begin{aligned} \dot{p}_i(t) &= v_i(t), \\ \dot{v}_i(t) &= - \sum_{j \in \mathcal{N}_i} P_{g_{ij}^*} [k_p (p_i(t) - p_j(t)) + k_v (v_i(t) - v_j(t))], \end{aligned} \quad (13)$$

where  $i \in \mathcal{V}_f$  and  $k_p, k_v$  are positive constant control gains. Under control law (13), the target formation is globally stable if it is bearing localizable.

If the velocities of the leaders are time varying, then the following control law requiring acceleration feedback can be used to track time-varying target formations [55]:

$$\begin{aligned} \dot{p}_i(t) &= v_i(t), \\ \dot{v}_i(t) &= K_i^{-1} \sum_{j \in \mathcal{N}_i} P_{g_{ij}^*} [-k_p (p_i(t) - p_j(t)) - k_v (v_i(t) - v_j(t)) + \dot{v}_j(t)], \end{aligned} \quad (14)$$

where  $i \in \mathcal{V}_f$  and  $K_i = \sum_{j \in \mathcal{N}_i} P_{g_{ij}^*}$ . The nonsingularity of  $K_i$  for any  $i \in \mathcal{V}_f$  is guaranteed by the bearing localizability of the target formation [55, Lemma 3]. Under (14), the target formation is globally stable if and only if it is bearing

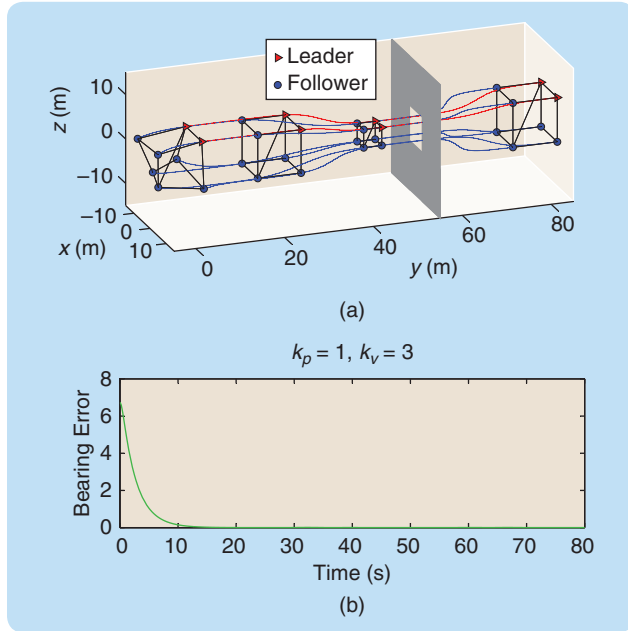


**FIGURE 11** A simulation example to demonstrate the bearing formation maneuvering control law in (14): (a) the generated formation maneuver trajectory (the dark area represents an obstacle) and (b) the total bearing error of the trajectory  $\sum_{(i,j) \in \mathcal{E}} \|g_{ij}(t) - g_{ij}^*\|$ . The target formation in the example is a 3D cube with two leaders and six followers. The translation and scale of the formation can continuously vary while the formation pattern is maintained as desired. This example demonstrates that formation scale control can be used for obstacle avoidance, such as passing through narrow passages.

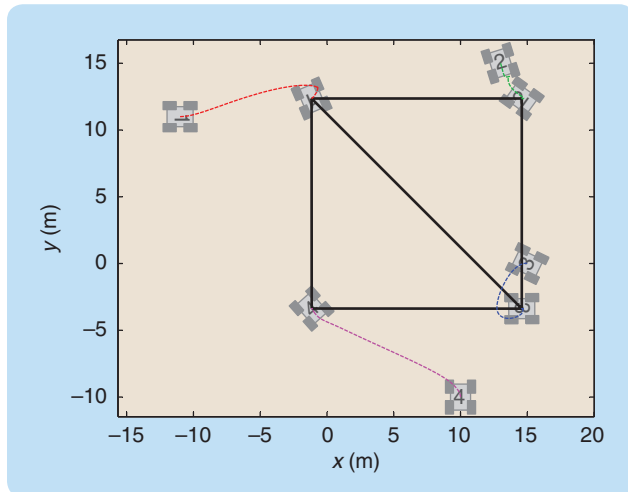


**FIGURE 12** A simulation example to demonstrate the control law in (16). In this example, there are four unicycle agents whose initial positions and heading angles are chosen randomly. As can be seen, the formation converges to the target formation whose square geometric pattern is defined by five bearing vectors.

localizable. A simulation example is given in Figure 11 to demonstrate (14). In practice, absolute acceleration can be measured by each agent using, for example, inertial measurement units and then transmitted to its neighbors by wireless communication. Because of measurement errors and transmission delays, the acceleration measurement is corrupted by errors. However, since the system is linear, bounded acceleration errors would cause bounded tracking errors. Bearing-based formation control in the presence of other problems (including input disturbance, input saturation, and collision avoidance) was addressed in [55].

### Bearing-Based Formation Control of Unicycles

Suppose the dynamics of agent  $i \in \mathcal{V}$  can be described by the unicycle model

$$\begin{aligned} \dot{x}_i &= v_i \cos \theta_i, \\ \dot{y}_i &= v_i \sin \theta_i, \\ \dot{\theta}_i &= w_i, \end{aligned} \quad (15)$$

where  $p_i = [x_i, y_i]^T \in \mathbb{R}^2$  is the coordinate of agent  $i$ ,  $\theta_i \in \mathcal{S}^1$  is the heading angle, and  $v_i \in \mathbb{R}$  and  $w_i \in \mathbb{R}$  are the linear and angular velocities, respectively, to be designed. Here,  $\mathcal{S}^1$  is the 1D manifold on the unit circle. The bearing-based formation control law for unicycles is [72]

$$\begin{aligned} v_i &= [\cos \theta_i \sin \theta_i] \sum_{j \in \mathcal{N}_i} P_{g_{ij}^*} (p_j(t) - p_i(t)), \\ w_i &= [-\sin \theta_i \cos \theta_i] \sum_{j \in \mathcal{N}_i} P_{g_{ij}^*} (p_j(t) - p_i(t)). \end{aligned} \quad (16)$$

When there are no leaders, (16) ensures global stability in the sense that  $g_{ij}(t)$  converges to either  $g_{ij}^*$  or  $-g_{ij}^*$  as  $t \rightarrow \infty$ , given any initial values of  $p_i(0)$  and  $\theta_i(0)$  if the target formation is infinitesimally bearing rigid [72]. The final value of  $\theta_i$  is not specified in the control law. A simulation example is shown in Figure 12.

### BEARING-ONLY FORMATION CONTROL

This section introduces the theory of bearing-only formation control, which studies how to steer a group of agents to achieve a bearing-constrained target formation using bearing-only measurements. Suppose the target formation is specified by constant bearing constraints  $\{g_{ij}^*\}_{(i,j) \in \mathcal{E}}$ , and there are no leaders. The control objective is to govern the positions of the agents  $\{p_i(t)\}_{i \in \mathcal{V}}$  such that  $g_{ij}(t) \rightarrow g_{ij}^*$  for all  $(i, j) \in \mathcal{E}$  as  $t \rightarrow \infty$ . All bearings are expressed in a common reference frame.

The following nonlinear control law, proposed in [28], can be used to solve the bearing-only formation control problem:

$$\dot{p}_i(t) = - \sum_{j \in \mathcal{N}_i} P_{g_{ij}(t)} g_{ij}^*, \quad i \in \mathcal{V}, \quad (17)$$

where  $P_{g_{ij}(t)} = I_d - g_{ij}(t)g_{ij}^T(t)$ . The geometric interpretation of the control law is illustrated in Figure 13. Some properties of the control law are highlighted below. First, the control of each agent requires only bearing measurements and no distance or position estimation. Second, the control input of (17) is always bounded as  $\|\dot{p}_i(t)\| \leq \sum_{j \in \mathcal{N}_i} \|P_{g_{ij}(t)}\| \|g_{ij}^*\| = |\mathcal{N}_i|$ , since  $\|P_{g_{ij}(t)}\| = \|g_{ij}^*\| = 1$ . Third, the centroid and scale of the formation are invariant under the control law [28, Th. 9]. Here, the centroid is defined as the average position of the agents, and the scale as the standard deviation of the distances from the

agents to the centroid. Simulation examples are given in Figures 14 and 15 to demonstrate (17).

Control law (17) is nonlinear and almost globally stable if the target formation is infinitesimally bearing rigid [28, Th. 11]. The term *almost* is due to the fact that there are two isolated equilibria of the error dynamics: desired and undesired. At the desired equilibrium, the bearings are equal to the desired values; that is,  $g_{ij} = g_{ij}^*$  for  $(i, j) \in \mathcal{E}$ . At the undesired equilibrium, the bearings are opposite to the desired values; that is,  $g_{ij} = -g_{ij}^*$  for  $(i, j) \in \mathcal{E}$ . The formations at the two equilibria have the same centroid and scale but opposite bearings. The almost global stability means that the formation would converge to the desired equilibrium unless the initial formation lies exactly on the undesired equilibrium, which can be shown to be an unstable one.

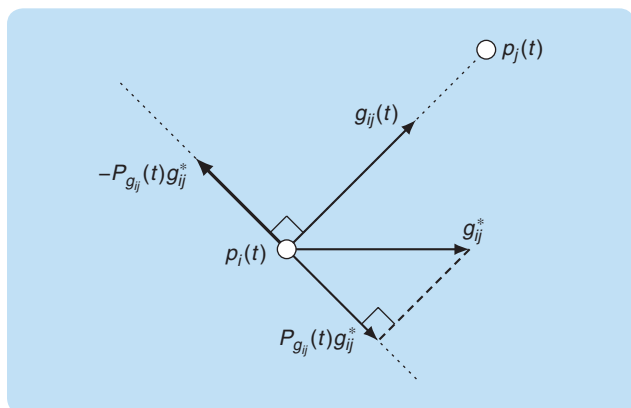


**FIGURE 13** The geometric interpretation of the bearing-only control law in (17). Since the control term  $-P_{g_{ij}}g_{ij}^*$  is perpendicular to the bearing  $g_{ij}$ , the control law aims to reduce the bearing error of  $g_{ij}(t)$  while maintaining the distance between agents  $i$  and  $j$ .

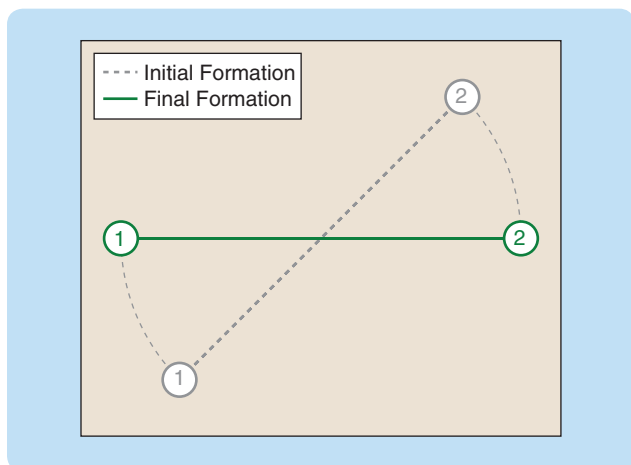


**FIGURE 14** A simulation example to demonstrate the bearing-only formation control law in (17). In this example, the formation has two agents and one edge. In the target formation, the bearings are in the horizontal direction; that is,  $g_{12}^* = -g_{21}^* = [1, 0]^T$ . The initial formation (dotted line) does not fulfill the desired bearings. Under the control law in (17), the formation converges to the desired one (solid line). Note that the velocity of each agent is always perpendicular to the bearing, and hence the two agents move on a circle centered at their midpoint. As a result, the centroid and scale of the formation are invariant.

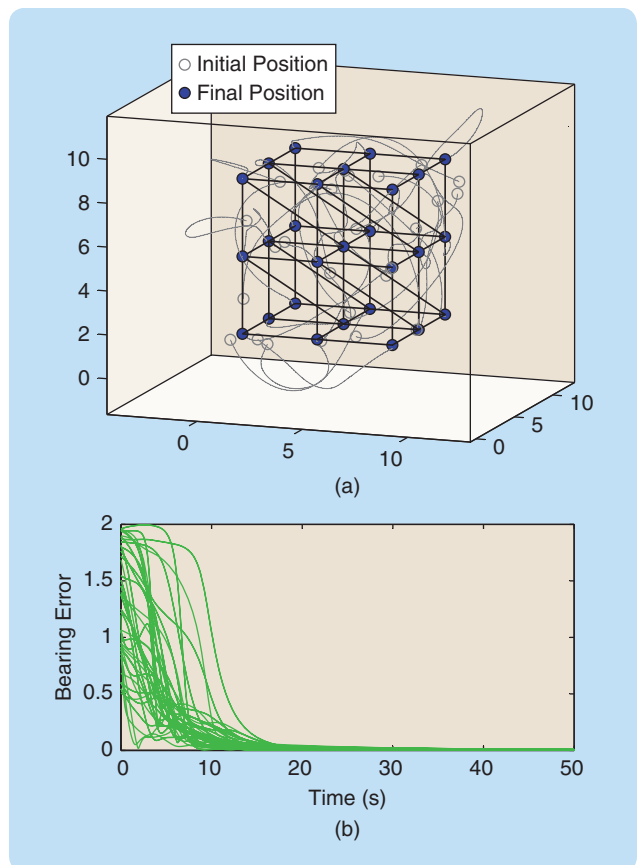


**FIGURE 15** A simulation example for the bearing control law in (17) in the 3D space: (a) the initial configuration (gray circles) and the final desired formation (blue circles) and (b) the plot of the bearing error  $\sum_{(i,j) \in \mathcal{E}} \|g_{ij}(t) - g_{ij}^*\|$ . In this example, the formation has 27 nodes and 62 edges. For the target formation, the rank of the bearing rigidity matrix, which equals the rank of the bearing Laplacian matrix, is  $3n - 4 = 77$ . As a result, the target formation is infinitesimally bearing rigid, and hence the control law (17) is almost globally stable. As can be seen, given a random initial configuration, the target formation is achieved and the bearing errors converge to zero.

Control law (17) is a modified gradient-descent control law. Consider the following objective function:

$$\phi_1 = \frac{1}{2} \sum_{(i,j) \in \mathcal{E}} \|g_{ij} - g_{ij}^*\|^2 = \sum_{(i,j) \in \mathcal{E}} (1 - g_{ij}^T g_{ij}^*).$$

The objective function is equal to zero if and only if  $g_{ij} = g_{ij}^*$  for all  $(i, j) \in \mathcal{E}$ . The corresponding gradient-descent control law is

$$\dot{p}_i(t) = - \sum_{j \in \mathcal{N}_i} \frac{1}{\|e_{ij}(t)\|} P_{g_{ij}(t)} g_{ij}^*, \quad i \in \mathcal{V}. \quad (18)$$

The 2D version of (18) was first proposed in [24]. This control law requires both bearing and distance measurements. Removing the distance term  $\|e_{ij}(t)\|$  in (18) yields the bearing-only formation control law in (17).

An optimization-based approach for bearing-only formation control can be found in [10] and [65], where a bearing-only control law is proposed as

$$\dot{p}_i(t) = \sum_{j \in \mathcal{N}_i} (g_{ij}(t) - g_{ij}^*), \quad i \in \mathcal{V}. \quad (19)$$

This is a gradient-descent control law with the corresponding objective function as

$$\phi_2 = \frac{1}{4} \sum_{(i,j) \in \mathcal{E}} \|e_{ij}\| \|g_{ij} - g_{ij}^*\|^2 = \frac{1}{2} \sum_{(i,j) \in \mathcal{E}} \|e_{ij}\| (1 - g_{ij}^T g_{ij}^*).$$

Since  $\phi_2$  contains  $\|e_{ij}\|$ ,  $\phi_2$  is zero when  $g_{ij} = g_{ij}^*$  or  $e_{ij} = 0$ . As a result, the scale of the formation always decreases under the action of control law (19). Simulation shows that this control law may steer all agents to the same position, given certain initial conditions. To avoid this problem, leaders must be introduced [65].

## CONCLUSIONS AND FUTURE DIRECTIONS

This article presented a review of bearing rigidity theory and its applications in distributed formation control and network localization for multiagent systems. Motivated by the fact that many existing approaches rely on measurement assumptions that may be difficult to realize under certain circumstances, this article demonstrated how to utilize bearing-only sensors, such as cameras or sensor arrays, to solve the problems of formation control and network localization. Three specific problems were discussed, including bearing-based network localization, bearing-based formation control, and bearing-only formation control.

The emerging research area of bearing-based control and estimation is far from being fully explored. Many important problems remain unsolved. One key assumption for the results presented here is that the underlying graph is undirected, which means any pair of neighbors must be able to access each other's information. Since this assumption may not be valid in practical tasks, it is important to study the case of directed graphs. When the graph is directed, the control and estimation problem would become more complicated because undesired equilibria may emerge, as observed in [68]. Similar problems also exist in distance-based formation control [73]–[75]. Despite the recent progress in bearing-only formation control for special directed graphs [76], [77], the problem for general directed graphs remains an important challenge in this area.

Another key assumption for the results in this article is that all bearings must be measured in a global reference frame. Global reference frames, however, may not be accessible to each agent in some environments, such as indoors. It is important to study how to achieve control or estimation when bearings are measured in each agent's local reference frames. One potential approach is to estimate or synchronize the orientations of the local reference frames [10], [28].

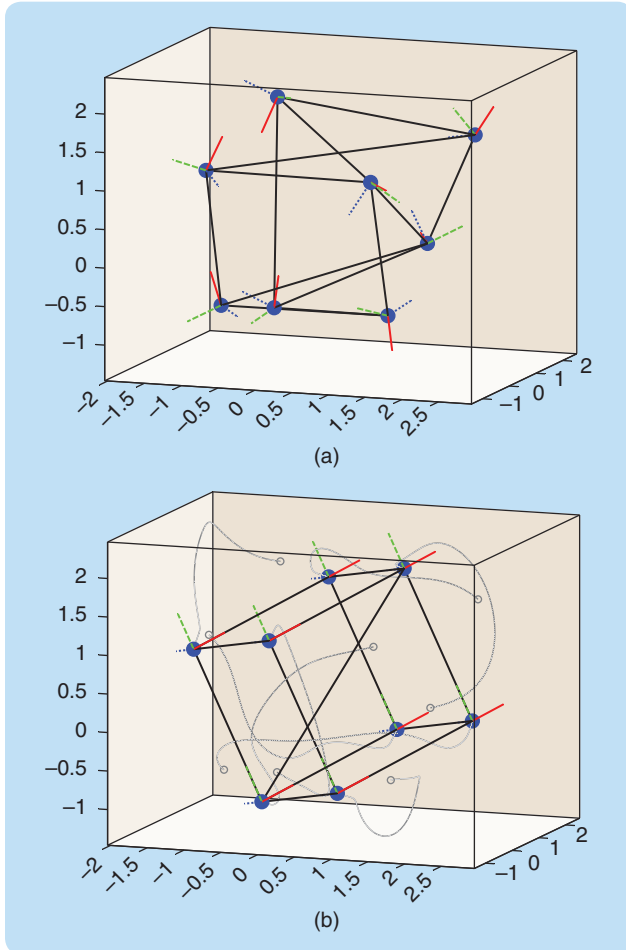


**FIGURE 16** A simulation example for bearing-only formation control without a global reference frame: (a) the initial formation and (b) the final formation. The control law is given in [28, eq. (19)]. In this example, the formation has eight nodes and 13 edges. The target formation is a 3D cube that is infinitesimally bearing rigid. The control is based on interneighbor bearings expressed in each agent's local reference frames. The orientations of the agents are synchronized in the final formation.

## Bearing Rigidity Theory for SE(2)

Consider a collection of  $n$  nodes in  $\mathbb{R}^2 \times \mathcal{S}^1$ . Each point is described by its position  $p_i \in \mathbb{R}^2$  and orientation  $\psi_i \in \mathcal{S}^1$ . An SE(2) network, denoted as  $(\mathcal{G}, \rho, \psi)$ , is the directed graph  $\mathcal{G} = (\mathcal{V}, \mathcal{E})$  and the configuration  $(\rho, \psi)$ , where each vertex  $i \in \mathcal{V}$  in the graph is mapped to the point  $(p_i, \psi_i) \in SE(2)$ . Note that with SE(2) networks, *directed* graphs are considered.

Suppose  $(i, j) \in \mathcal{E}$  is the  $k$ th directed edge, where  $k = \{1, \dots, m\}$ , and  $m$  denotes the number of directed edges in  $\mathcal{E}$ . Let  $g_k$  be the relative bearing of  $p_j$  with respect to  $p_i$  expressed in the global frame. Then,

$$r_k = \begin{bmatrix} \cos \psi_i & \sin \psi_i \\ -\sin \psi_i & \cos \psi_i \end{bmatrix} g_k$$

is the bearing  $g_k$  expressed in node  $i$ 's local reference frame. Define the directed bearing function associated with the SE(2) network,  $F_{SE}: SE(2)^n \rightarrow \mathcal{S}^{2m}$ , as

$$F_{SE}(\rho, \psi) = [r_1^T \cdots r_m^T]^T \in \mathcal{S}^{2m}. \quad (S3)$$

The corresponding directed bearing rigidity matrix is defined as the Jacobian of the directed bearing function

$$R_{SE}(\rho, \psi) \triangleq \frac{\partial F_{SE}(\rho, \psi)}{\partial (\rho, \psi)} \in \mathbb{R}^{2m \times 3n}. \quad (S4)$$

Let  $\delta\chi \in \mathbb{R}^{3n}$  be a variation of the configuration  $(\rho, \psi)$ . If  $R_{SE}(\rho, \psi)\delta\chi = 0$ , then  $\delta\chi$  is an infinitesimal SE(2) bearing motion of  $\mathcal{G}(\rho, \psi)$ . There are three types of trivial infinitesimal SE(2) motions corresponding to translations, scalings, and coordinated rotations of the entire network. The coordinated rotation involves an angular rotation of each agent about its own body axis with a rigid-body rotation of the network (see Figure S6). An SE(2) network is infinitesimally bearing rigid if all infinitesimal bearing motions are trivial. A necessary and

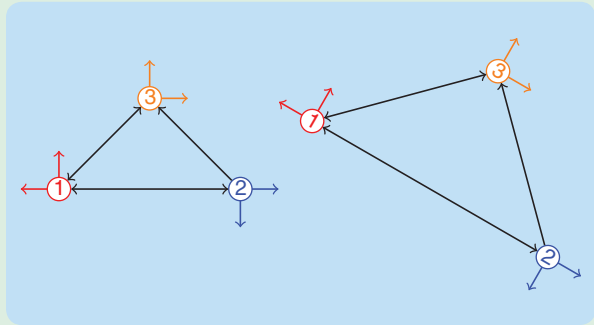


**FIGURE S6** An example of two congruent SE(2) networks. The above two networks differ in terms of translation, scaling, and coordinated rotation.

sufficient condition for an SE(2) network to be infinitesimally bearing rigid is [80], [81]

$$\text{rank}[R_{SE}(\rho, \psi)] = 3n - 4,$$

or, equivalently,

$$\text{Null}[R_{SE}(\rho, \psi)] = \text{span} \left\{ \begin{bmatrix} \mathbf{1}_n \otimes I_2 \\ 0 \end{bmatrix}, \begin{bmatrix} \rho \\ 0 \end{bmatrix}, \begin{bmatrix} \rho^\perp \\ \mathbf{1}_n \end{bmatrix} \right\},$$

where  $\rho^\perp = [(p_1^\perp)^T, \dots, (p_n^\perp)^T]^T$  and  $\rho^\perp = R_{\pi/2}\rho$ . The null space is characterized in this way after a permutation of the matrix that groups the positions and attitudes of all of the agents together. Here,  $R_{\pi/2}$  is a rotation matrix that rotates any vector by  $\pi/2$ .

Detailed definitions in the SE(2) bearing rigidity theory can be found in [26], [80], and [81]. The SE(2) rigidity theory has been employed for distributed relative position estimation [26] and formation control [80], [81], [83]. A similar approach has been extended for SE(3) [82].

This approach has been applied to adapt the bearing-only formation control law in (17) to use locally measured bearings [28, Sec. IV], and a simulation example is given in Figure 16. This is also a general approach for many types of formation control and network localization tasks in the absence of global reference frames [78], [79]. However, distributed orientation estimation or synchronization requires each agent to obtain its neighbors' relative orientations, which are usually difficult to measure in practice.

Other potential approaches that do not require an orientation estimation may be based on bearing rigidity in the special Euclidean group SE(n) [26], [80]–[83] or complex Laplacian [52], [57]. A brief introduction to bearing rigidity in SE(2) is given in "Bearing Rigidity Theory for SE(2)." Nevertheless, the formation control strategies provided for SE(2) frameworks still require additional sensing [80], and a complete theory for bearing-only formation control is still unsolved.

In addition to network localization and formation control, many other tasks may also be achieved with bearing-only measurements, such as bearing-only rendezvous [84]–[88], and bearing-only target tracking [16]–[18], [89], [90], although the analysis of these tasks may not rely on bearing rigidity theory.

Bearing rigidity theory and its application to formation control and network localization are strongly motivated by the sensing mediums available to distributed and multi-agent systems. This work contributed to the broader theory of cooperative control and estimation for networked systems and hopes to serve as a starting point for both practitioners and theoreticians in this community.

### AUTHOR INFORMATION

**Shiyu Zhao** (zhaoshiyu@westlake.edu.cn) is an assistant professor at Westlake University, Hangzhou, China. He received the B.E. and M.E. degrees from the Beijing University

of Aeronautics and Astronautics in 2006 and 2009, respectively, and the Ph.D. degree in electrical engineering from the National University of Singapore in 2014. From 2014 to 2016, he was a postdoctoral researcher at the Technion–Israel Institute of Technology, Haifa, and University of California, Riverside. From 2016 to 2018, he was a lecturer in the Department of Automatic Control and Systems Engineering, University of Sheffield, United Kingdom. He was a corecipient of the Best Paper Award (Guan Zhao-Zhi Award) in the 33rd Chinese Control Conference in 2014. He is currently an associate editor of *Unmanned Systems*. His research interests lie in networked dynamical systems and their applications to intelligent and robotic systems.

**Daniel Zelazo** is an associate professor of aerospace engineering at the Technion–Israel Institute of Technology, Haifa. He received the B.Sc. and M.Eng. degrees in electrical engineering and computer science from the Massachusetts Institute of Technology, Cambridge, in 1999 and 2001, respectively. Before beginning his doctoral studies, he worked for two years on audio compression algorithms as a research engineer at Texas Instruments, Japan. In 2009, he completed his Ph.D. degree at the University of Washington, Seattle, in aeronautics and astronautics. From 2010 to 2012, he was a postdoctoral research associate and lecturer at the Institute for Systems Theory and Automatic Control, University of Stuttgart, Germany. He is currently an associate editor of *IEEE Control Systems Letters*. His research interests include topics related to multiagent systems, optimization, and graph theory.

## REFERENCES

- [1] Y. Cao, W. Yu, W. Ren, and G. Chen, "An overview of recent progress in the study of distributed multi-agent coordination," *IEEE Trans. Ind. Inform.*, vol. 9, no. 1, pp. 427–438, 2013.
- [2] K.-K. Oh, M.-C. Park, and H.-S. Ahn, "A survey of multi-agent formation control," *Automatica*, vol. 53, pp. 424–440, Mar. 2015.
- [3] I. F. Akyildiz, W. Su, Y. Sankarasubramaniam, and E. Cayirci, "A survey on sensor networks," *IEEE Commun. Mag.*, vol. 40, pp. 102–114, Aug. 2002.
- [4] J. Aspnes et al., "A theory of network localization," *IEEE Trans. Mobile Comput.*, vol. 5, no. 12, pp. 1663–1678, 2006.
- [5] G. Mao, B. Fidan, and B. D. O. Anderson, "Wireless sensor network localization techniques," *Comput. Netw.*, vol. 51, no. 10, pp. 2529–2553, 2007.
- [6] P. Barooah and J. P. Hespanha, "Estimation on graphs from relative measurements," *IEEE Control Syst. Mag.*, no. 1, pp. 57–74, Aug. 2007.
- [7] Y. Ma, S. Soatto, J. Kosecka, and S. Sastry, *An Invitation to 3D Vision*. New York: Springer-Verlag, 2004.
- [8] R. I. Hartley and P. Sturm, "Triangulation," *Comput. Vision Image Understanding*, vol. 68, no. 2, pp. 146–157, 1997.
- [9] N. Moshtagh, N. Michael, A. Jadbabaie, and K. Daniilidis, "Vision-based, distributed control laws for motion coordination of nonholonomic robots," *IEEE Trans. Robot.*, vol. 25, pp. 851–860, Aug. 2009.
- [10] R. Tron, J. Thomas, G. Loianno, K. Daniilidis, and V. Kumar, "A distributed optimization framework for localization and formation control: Applications to vision-based measurements," *IEEE Control Syst. Mag.*, vol. 36, no. 4, pp. 22–44, 2016.
- [11] A. Farina, "Target tracking with bearings-only measurements," *Signal Process.*, vol. 78, no. 1, pp. 61–68, 1999.
- [12] Y.-Y. Dong, C.-X. Dong, W. Liu, H. Chen, and G.-Q. Zhao, "2-D DOA estimation for L-shaped array with array aperture and snapshots extension techniques," *IEEE Signal Process. Lett.*, vol. 24, no. 4, pp. 495–499, 2017.
- [13] G. Stacey and R. Mahony, "A passivity-based approach to formation control using partial measurements of relative position," *IEEE Trans. Autom. Control*, vol. 61, no. 2, pp. 538–543, 2016.
- [14] K. Becker, "Simple linear theory approach to TMA observability," *IEEE Trans. Aerosp. Electron. Syst.*, vol. 29, no. 2, pp. 575–578, 1993.
- [15] M. Deghat, I. Shames, B. D. O. Anderson, and C. Yu, "Localization and circumnavigation of a slowly moving target using bearing measurements," *IEEE Trans. Autom. Control*, vol. 59, no. 8, pp. 2182–2188, 2014.
- [16] J. O. Swartling, I. Shames, K. H. Johansson, and D. V. Dimarogonas, "Collective circumnavigation," *Unmanned Syst.*, vol. 2, no. 3, pp. 219–229, 2014.
- [17] R. Zheng, Y. Liu, and D. Sun, "Enclosing a target by nonholonomic mobile robots with bearing-only measurements," *Automatica*, vol. 53, pp. 400–407, Mar. 2015.
- [18] M. Ye, B. D. O. Anderson, and C. Yu, "Bearing-only measurement self-localization, velocity consensus and formation control," *IEEE Trans. Aerosp. Electron. Syst.*, vol. 52, no. 2, pp. 575–586, 2017.
- [19] R. Olfati-Saber and R. M. Murray, "Consensus problems in networks of agents with switching topology and time-delays," *IEEE Trans. Autom. Control*, vol. 49, no. 9, pp. 1520–1533, 2004.
- [20] Z. Lin, B. Francis, and M. Maggiore, "Necessary and sufficient graphical conditions for formation control," *IEEE Trans. Autom. Control*, vol. 50, pp. 121–127, Jan. 2005.
- [21] W. Ren, R. W. Beard, and E. M. Atkins, "Information consensus in multi-vehicle cooperative control," *IEEE Control Syst. Mag.*, vol. 27, pp. 71–82, Apr. 2007.
- [22] Z. Li, Z. Duan, G. Chen, and L. Huang, "Consensus of multiagent systems and synchronization of complex networks: A unified viewpoint," *IEEE Trans. Circuits Syst. I*, vol. 57, no. 1, pp. 213–224, 2010.
- [23] B. Servatius and W. Whiteley, "Constraining plane configurations in computer-aided design: Combinatorics of directions and lengths," *SIAM J. Discrete Math.*, vol. 12, no. 1, pp. 136–153, 1999.
- [24] A. N. Bishop, "Stabilization of rigid formations with direction-only constraints," in *Proc. 50th IEEE Conf. Decision and Control and Eur. Control Conf.*, Orlando, FL, 2011, pp. 746–752.
- [25] T. Eren, "Formation shape control based on bearing rigidity," *Int. J. Control*, vol. 85, no. 9, pp. 1361–1379, 2012.
- [26] D. Zelazo, A. Franchi, and P. R. Giordano, "Rigidity theory in SE(2) for unscaled relative position estimation using only bearing measurements," in *Proc. Eur. Control Conf.*, Strasbourg, France, 2014, pp. 2703–2708.
- [27] R. Tron, L. Carlone, F. Dellaert, and K. Daniilidis, "Rigid components identification and rigidity control in bearing-only localization using the graph cycle basis," in *Proc. Amer. Control Conf.*, Chicago, IL, 2015, pp. 3911–3918.
- [28] S. Zhao and D. Zelazo, "Bearing rigidity and almost global bearing-only formation stabilization," *IEEE Trans. Autom. Control*, vol. 61, no. 5, pp. 1255–1268, 2016.
- [29] L. Asimow and B. Roth, "The rigidity of graphs," *Trans. Amer. Math. Soc.*, vol. 245, pp. 279–289, Nov. 1978.
- [30] R. Connelly and S. D. Guest, "Frameworks, tensegrities, and symmetry: Understanding stable structures," Cornell University, College of Arts and Sciences, May 22, 2015. [Online]. Available: <http://www.math.cornell.edu/~web7510/framework.pdf>
- [31] B. Hendrickson, "Conditions for unique graph realizations," *SIAM J. Computing*, vol. 21, no. 1, pp. 65–84, 1992.
- [32] R. Connelly, "Generic global rigidity," *Discrete Computational Geometry*, vol. 33, no. 4, pp. 549–563, 2005.
- [33] D. Jacobs, "An algorithm for two-dimensional rigidity percolation: The pebble game," *Comput. Phys.*, vol. 137, pp. 346–365, Nov. 1997.
- [34] T.-S. Tay and W. Whiteley, "Generating isostatic frameworks," *Structural Topology*, vol. 11, pp. 21–69, 1985.
- [35] R. Haas et al., "Planar minimally rigid graphs and pseudo-triangulations," *Computational Geometry*, vol. 31, no. 1–2, pp. 31–61, 2005.
- [36] B. Jackson, "Notes on the rigidity of graphs," School Math. Sci., Queen Mary Univ. London, Tech. Rep., 2007.
- [37] B. D. O. Anderson, C. Yu, B. Fidan, and J. Hendrickx, "Rigid graph control architectures for autonomous formations," *IEEE Control Syst. Mag.*, vol. 28, pp. 48–63, Dec. 2008.
- [38] L. Krick, M. E. Broucke, and B. A. Francis, "Stabilization of infinitesimally rigid formations of multi-robot networks," *Int. J. Control*, vol. 82, no. 3, pp. 423–439, 2009.
- [39] K.-K. Oh and H.-S. Ahn, "Distance-based undirected formations of single-integrator and double-integrator modeled agents in n-dimensional space," *Int. J. Robust Nonlinear Control*, vol. 24, pp. 1809–1820, Aug. 2014.
- [40] Y.-P. Tian and Q. Wang, "Global stabilization of rigid formations in the plane," *Automatica*, vol. 49, pp. 1436–1441, May 2013.
- [41] D. Zelazo, A. Franchi, and P. R. Giordano, "Distributed rigidity maintenance control with range-only measurements for multi-robot systems," *Int. J. Robot. Res.*, vol. 34, no. 1, pp. 105–128, 2015.

- [42] S. Mou, M.-A. Belabbas, A. S. Morse, Z. Sun, and B. D. O. Anderson, "Undirected rigid formations are problematic," *IEEE Trans. Autom. Control*, vol. 61, no. 10, pp. 2821–2836, 2016.
- [43] X. Chen, M.-A. Belabbas, and T. Başar, "Global stabilization of triangulated formations," *SIAM J. Optimization Control*, vol. 55, no. 1, pp. 172–199, 2017.
- [44] Z. Sun, M.-C. Park, B. D. O. Anderson, and H.-S. Ahn, "Distributed stabilization control of rigid formations with prescribed orientation," *Automatica*, vol. 78, pp. 250–257, Apr. 2017.
- [45] H. G. de Marina, B. Jayawardhana, and M. Cao, "Distributed rotational and translational maneuvering of rigid formations and their applications," *IEEE Trans. Robot.*, vol. 32, no. 3, pp. 684–697, 2016.
- [46] T. Eren et al., "Rigidity, computation, and randomization in network localization," in *23rd Annu. Joint Conf. IEEE Computer and Communications Societies*, Pasadena, CA, 2004, pp. 2673–2684.
- [47] T. Eren, W. Whiteley, A. S. Morse, P. N. Belhumeur, and B. D. O. Anderson, "Sensor and network topologies of formations with direction, bearing and angle information between agents," in *Proc. 42nd IEEE Conf. Decision and Control*, 2003, pp. 3064–3069.
- [48] A. N. Bishop, B. D. O. Anderson, B. Fidan, P. N. Pathirana, and G. Mao, "Bearing-only localization using geometrically constrained optimization," *IEEE Trans. Aerosp. Electron. Syst.*, vol. 45, no. 1, pp. 308–320, 2009.
- [49] G. Piovan, I. Shames, B. Fidan, F. Bullo, and B. D. O. Anderson, "On frame and orientation localization for relative sensing networks," *Automatica*, vol. 49, pp. 206–213, Jan. 2013.
- [50] I. Shames, A. N. Bishop, and B. D. O. Anderson, "Analysis of noisy bearing-only network localization," *IEEE Trans. Autom. Control*, vol. 58, pp. 247–252, Jan. 2013.
- [51] G. Zhu and J. Hu, "A distributed continuous-time algorithm for network localization using angle-of-arrival information," *Automatica*, vol. 50, pp. 53–63, Jan. 2014.
- [52] Z. Lin, T. Han, R. Zheng, and M. Fu, "Distributed localization for 2-D sensor networks with bearing-only measurements under switching topologies," *IEEE Trans. Signal Process.*, vol. 64, no. 23, pp. 6345–6359, 2016.
- [53] A. N. Bishop, M. Deghat, B. D. O. Anderson, and Y. Hong, "Distributed formation control with relaxed motion requirements," *Int. J. Robust Nonlinear Control*, vol. 25, no. 17, pp. 3210–3230, 2015.
- [54] S. Zhao and D. Zelazo, "Bearing-based distributed control and estimation in multi-agent systems," in *Proc. Eur. Control Conf.*, Linz, Austria, 2015, pp. 2207–2212.
- [55] S. Zhao and D. Zelazo, "Translational and scaling formation maneuver control via a bearing-based approach," *IEEE Trans. Control Netw. Syst.*, vol. 4, no. 3, pp. 429–438, 2017.
- [56] K. Fathian, D. I. Rachinskii, M. W. Spong, and N. R. Gans, "Globally asymptotically stable distributed control for distance and bearing based multi-agent formations," in *Proc. 2016 Amer. Control Conf.*, Boston, MA, 2016, pp. 4642–4648.
- [57] Z. Han, L. Wang, Z. Lin, and R. Zheng, "Formation control with size scaling via a complex Laplacian-based approach," *IEEE Trans. Cybern.*, vol. 46, no. 10, pp. 2348–2359, 2016.
- [58] S. Coogan and M. Arcaç, "Scaling the size of a formation using relative position feedback," *Automatica*, vol. 48, pp. 2677–2685, Oct. 2012.
- [59] M. Basiri, A. N. Bishop, and P. Jensfelt, "Distributed control of triangular formations with angle-only constraints," *Syst. Control Lett.*, vol. 59, no. 2, pp. 147–154, 2010.
- [60] A. Franchi, C. Masone, V. Grabe, M. Ryll, H. H. Bulthoff, and P. R. Giordano, "Modeling and control of UAV bearing formations with bilateral high-level steering," *Int. J. Robot. Res.*, vol. 31, no. 12, pp. 1504–1525, 2012.
- [61] A. Cornejo, A. J. Lynch, E. Fudge, S. Bilstein, M. Khabbazi, and J. McLurkin, "Scale-free coordinates for multi-robot systems with bearing-only sensors," *Int. J. Robot. Res.*, vol. 32, no. 12, pp. 1459–1474, 2013.
- [62] S. Zhao, F. Lin, K. Peng, B. M. Chen, and T. H. Lee, "Distributed control of angle-constrained cyclic formations using bearing-only measurements," *Syst. Control Lett.*, vol. 63, no. 1, pp. 12–24, 2014.
- [63] S. Zhao, F. Lin, K. Peng, B. M. Chen, and T. H. Lee, "Finite-time stabilization of cyclic formations using bearing-only measurements," *Int. J. Control*, vol. 87, no. 4, pp. 715–727, 2014.
- [64] E. Schoof, A. Chapman, and M. Mesbahi, "Bearing-compass formation control: A human-swarm interaction perspective," in *Proc. Amer. Control Conf.*, Portland, OR, 2014, pp. 3881–3886.
- [65] R. Tron, J. Thomas, G. Loianno, K. Daniilidis, and V. Kumar, "Bearing-only formation control with auxiliary distance measurements, leaders, and collision avoidance," in *Proc. 55th Conf. Decision and Control*, Las Vegas, NV, 2016, pp. 1806–1813.
- [66] S. Zhao and D. Zelazo, "Localizability and distributed protocols for bearing-based network localization in arbitrary dimensions," *Automatica*, vol. 69, pp. 334–341, July 2016.
- [67] C. Godsil and G. Royle, *Algebraic Graph Theory*. New York: Springer-Verlag, 2001.
- [68] S. Zhao and D. Zelazo, "Bearing-based formation stabilization with directed interaction topologies," in *Proc. 54th IEEE Conf. Decision and Control*, Osaka, Japan, 2015, pp. 6115–6120.
- [69] S. Zhao, Z. Sun, D. Zelazo, M. H. Trinh, and H.-S. Ahn, "Laman graphs are generically bearing rigid in arbitrary dimensions," in *Proc. 56th IEEE Conf. Decision and Control*, Melbourne, Australia, 2017. [Online]. Available: [arxiv:abs/1703.04035](https://arxiv.org/abs/1703.04035)
- [70] G. Laman, "On graphs and rigidity of plane skeletal structures," *J. Eng. Math.*, vol. 4, no. 4, pp. 331–340, 1970.
- [71] S. Zhao and D. Zelazo, "Bearing-based formation maneuvering," in *Proc. IEEE Multi-Conf. Systems and Control*, Sydney, Australia, 2015, pp. 658–663.
- [72] S. Zhao, D. V. Dimarogonas, Z. Sun, and D. Bauso, "A general approach to coordination control of mobile agents with motion constraints," *IEEE Trans. Autom. Control*, vol. 63, no. 5, pp. 1509–1516, 2018. doi: 10.1109/TAC.2017.2750924.
- [73] J. Hendrickx, B. D. O. Anderson, J. Delvenne, and V. Blondel, "Directed graphs for the analysis of rigidity and persistence in autonomous agent systems," *Int. J. Robust Nonlinear Control*, vol. 17, no. 10–11, pp. 960–981, 2007.
- [74] C. Yu, B. D. O. Anderson, A. S. Dasgupta, and B. Fidan, "Control of minimally persistent formations in the plane," *SIAM J. Control Optimization*, vol. 48, pp. 206–233, Feb. 2009.
- [75] T. H. Summers, C. Yu, S. Dasgupta, and B. D. O. Anderson, "Control of minimally persistent leader-remote-follower and coleader formations in the plane," *IEEE Trans. Autom. Control*, vol. 56, no. 12, pp. 2778–2792, 2011.
- [76] D. Mukherjee, M.-H. Trinh, D. Zelazo, and H.-S. Ahn, "Bearing-only cyclic pursuit in 2-D for capture of moving target," in *Proc. 57th Israel Annu. Conf. Aerospace Sciences*, Haifa, Israel, 2017.
- [77] M.-H. Trinh, D. Mukherjee, D. Zelazo, and H.-S. Ahn, "Formations on directed cycles with bearing-only measurements," *Int. J. Robust Nonlinear Control*, vol. 28, no. 3, pp. 1074–1096, 2018. doi: 10.1002/rnc.3921.
- [78] K.-K. Oh and H.-S. Ahn, "Formation control and network localization via orientation alignment," *IEEE Trans. Autom. Control*, vol. 59, pp. 540–545, Feb. 2014.
- [79] B.-H. Lee and H.-S. Ahn, "Distributed formation control via global orientation estimation," *Automatica*, vol. 73, pp. 125–129, Nov. 2016.
- [80] D. Zelazo, A. Franchi, and P. R. Giordano, "Formation control using a SE(2) rigidity theory," in *Proc. 54th IEEE Conf. Decision and Control*, Osaka, Japan, 2015, pp. 6121–6126.
- [81] F. Schiano, A. Franchi, D. Zelazo, and P. R. Giordano, "A rigidity-based decentralized bearing formation controller for groups of quadrotor UAVs," in *Proc. IEEE/RSJ Int. Conf. Intelligent Robots and Systems*, Daejeon, South Korea, 2016, pp. 5099–5106.
- [82] G. Michieletto, A. Cenedese, and A. Franchi, "Bearing rigidity theory in SE(3)," in *Proc. 55th IEEE Conf. Decision and Control*, 2016, pp. 83–92.
- [83] F. Schiano and P. G. Robuffo, "Bearing rigidity maintenance for formations of quadrotor UAVs," in *Proc. IEEE Int. Conf. Robotics and Automation*, Singapore, 2017, pp. 1467–1474.
- [84] J. Yu, S. M. LaValle, and D. Liberzon, "Rendezvous without coordinations," *IEEE Trans. Autom. Control*, vol. 57, no. 2, pp. 421–434, 2012.
- [85] R. Zheng and D. Sun, "Rendezvous of unicycles: A bearings-only and perimeter shortening approach," *Syst. Control Lett.*, vol. 62, pp. 401–407, May 2013.
- [86] J. Grzymisch and W. Fichter, "Optimal rendezvous guidance with enhanced bearings-only observability," *J. Guidance, Control, Dynamics*, vol. 38, no. 6, pp. 1131–1139, 2015.
- [87] M. Krieglleder, S. T. Digumarti, R. Oung, and R. D'Andrea, "Rendezvous with bearing-only information and limited sensing range," in *Proc. IEEE Int. Conf. Robotics and Automation*, Seattle, Washington, 2015, pp. 5941–5947.
- [88] S. Zhao and R. Zheng, "Flexible bearing-only rendezvous control of mobile robots," in *Proc. 36th Chinese Control Conf.*, Dalian, China, 2017, pp. 8051–8056.
- [89] S. G. Loizou and V. Kumar, "Biologically inspired bearing-only navigation and tracking," in *Proc. 46th IEEE Conf. Decision and Control*, New Orleans, LA, 2007, pp. 1386–1391.
- [90] M.-H. Trinh, G.-H. Ko, V.-H. Pham, K.-K. Oh, and H.-S. Ahn, "Guidance using bearing-only measurements with three beacons in the plane," *Control Eng. Practice*, vol. 51, pp. 81–91, June 2016.